



Delineation of groundwater potential zones using the AHP technique: a case study of Alipurduar district, West Bengal

Saumyajit Ghosh¹ · Dipankar Das² · Shasanka Kumar Gayen² · Pankaj Bhardwaj³

Received: 21 October 2022 / Accepted: 7 February 2023 / Published online: 20 March 2023
© The Author(s), under exclusive licence to Springer Nature Switzerland AG 2023

Abstract

Increasing population with increasing demand of groundwater affects the level of groundwater. In the context of considerable change in the use of groundwater pattern, particularly with continuous increase in demand for groundwater due to many reasons, the present paper attempts to delineate groundwater potential zones (GWPZ) using integrated remote sensing, geographic information systems (GIS) and analytic hierarchy process (AHP) methods. To transform and harmonize geographic data and weightage ranking to get reliable information, geographic information systems are combined with analytical hierarchical processes. The current study has been done in the district where many areas are under tea garden and cultivated land. The use of excess of groundwater results in a drop in the water level. The mapping and the identification of groundwater potential zones were done for the Ganga alluvial plain of Alipurduar District of India. The groundwater potential index (GPI) was computed based on several factors (e.g., land use–land cover, soil type, geology, elevation, slope, rainfall, normalized difference vegetation index, drainage density, pre- and post-monsoon groundwater depth, etc.). To generate the groundwater potential zone map of the study area, an overlay weighted sum method was applied to integrate all thematic criteria. Groundwater potential index maps have been classified into five zones. The excellent potential zone comprise 50.5% (1583.68 km²), good 27.4% (859.26 km²), moderate 11.3% (354.37 km²), poor 7.1% (222.66 km²) and very poor 3.7% (116.03 km²), respectively. After that, the maps were verified with groundwater-level fluctuation data of 30 observed wells through the ROC (receivers operating characteristic) curve. This paper has important implications for planning the sustainable groundwater plan and also different purposes, such as natural and artificial recharge, watershed delineation and proper water usage, can be effectively implemented in this agriculture-dominated areas in the district.

Keywords GIS techniques · Groundwater potential zone · Alipurduar · ROC · Weighted overlay

Introduction

In addition to being essential for human survival, groundwater is crucial for global food security, economic development, and population expansion. Groundwater resources are currently in danger of being inaccessible owing to overexploitation and inadequate management techniques. Throughout the planet, there is uneven distribution of groundwater. Also, it supports the survival of numerous people and is the only source of drinking water. The influence of groundwater from agricultural irrigation to industrial irrigation is massive and significant in the world. According to assessments conducted (IPCC 2018) at the worldwide level, basins are considered to be water stressed if their per capita water availability is less than 1,000 m³ per year (based on long-term average runoff) or if their ratio of withdrawals to

✉ Saumyajit Ghosh
saumyajitghosh1993@gmail.com

Dipankar Das
dasdipankar783@gmail.com

Shasanka Kumar Gayen
gshasanka@gmail.com

Pankaj Bhardwaj
pkbhardwaj007@gmail.com

¹ Department of Geography, State Aided College Teacher, Cooch Behar College, Cooch Behar, India

² Department of Geography, Cooch Behar Panchanan Barma University, Cooch Behar, India

³ Department of Geography, Government College Bahu, Jhajjar, Haryana, India

long-term average annual runoff is more than 0.4. Typically, 1,000 m³ of water per person per year is more than sufficient for home, industrial, and agricultural water demands. Northern Africa, the Mediterranean region, the Middle East, the Near East, southern Asia, northern China, Australia, the USA, Mexico, Northeastern Brazil, and the west coast of South America are among the regions with such water-stressed basins withdrawals globally and for almost 90% of consumptive water use (i.e., the water volume that is not available for reuse downstream). About 70% of all water is used for irrigation. Groundwater plays a leading role in keeping up with environmental equilibrium, human prosperity and monetary turn of events (IPCC 2001). So, it is fundamental to both growth in the economy and agricultural production. Globally, residential, rural, and urban uses account for approximately 36%, 42%, and 27% of total groundwater extraction, respectively (Taylor et al. 2013). An investigation conducted in the USA revealed that groundwater levels in the Californian San Joaquin Valley have decreased by 60–150 cm over the previous 5 years. Based on the four climate scenarios, northeastern Brazil, southwestern Africa, and the southern Mediterranean Sea rim all experience substantial reductions in groundwater recharge of more than 70% (Kundzewicz et al. 2007; Do et al. 2005). By the mid-2050s, groundwater recharge in the Sahel, the Near East, Northern China, Siberia, and the western USA will increase by more than 30%. It is very likely that Asia will become warmer during the twenty-first century, and this warming may differ by region. For instance, central Asia, the Tibetan Plateau, and northern Asia may experience temperatures that are significantly higher than the global mean, while East and South Asia and Southeast Asia may experience temperatures that are similar to the global mean. In a nation like India, 90% of the provincial population and 30% of metropolitan individuals rely upon groundwater to satisfy their fundamental prerequisites (Agarwal and Garg 2016). According to NASA's Gravity Recovery and Climate Experiment (GRACE) twin satellites, the groundwater level is dropping by 33 cm per year in the Indian states of Rajasthan, Punjab, and Haryana (Rodell et al. 2009). As a result of population expansion, which is anticipated to be impacted by spatiotemporal precipitation variability, it is predicted that the gross per capita water availability in India will decrease from roughly 1,820 m³/year in 2001 to as little as 1,140 m³/year in 2050 (Gupta and Deshpande 2004). Sadly, shortage and widespread utilization of groundwater assets without proper logical arranging are exceptionally recognizable situation in India (Rodell et al. 2009). Due to an increase in groundwater extraction over the past 20 years, several areas of India have seen rapidly dropping groundwater

levels (CWC and CGWB 2016). Changes in land use and land cover, urbanization, and pollution all have an impact on groundwater recharge. Loss of forest cover, modifications to cropping practices and rotation, and long-term changes to soil characteristics may have an impact on infiltration capacity. This is crucial because its occurrence, initiation, appropriation, and development are dependent on topographical arrangement (such as lithology, thickness, layout, and spring penetrability), climate, geomorphologic features, topsoil, ground incline, patterns of land use or land cover, force of waste, and their interactions with the hydrodynamic feature (Krishnamurthy and Srinivas 1995; Greenbaum 1992; Saraf and Choudhury 1998; Schultz and Engman 2012; Taylor et al. 2013; Ebrahimi et al. 2016).

Besides, different strategies have been used by different analysts; for example, choice tree model (Lee and Lee 2015), recurrence proportion (Guru et al. 2017; Al-Abadi et al. 2016), loads of proof (GhorbaniNejad et al. 2017; Madani and Niyazi 2015), fake brain organization (Lee et al. 2017), arbitrary backwoods model (Naghbi et al. 2016), calculated relapse model (Pourtaghi and Pourghasemi 2014), evidential conviction work (Nampak et al. 2014), and so on. A considerable number of the current examinations (Jasrotia et al. 2016; Mallick et al. 2015; Gumma and Pavelic 2013; Chenini et al. 2010; Madrucci et al. 2008; Srivastava and Bhattacharya 2006; Sikdar et al. 2004; Krishnamurthy et al. 1996) have generally applied RS and GIS strategies for the appraisal of groundwater potential zone (GWPZ). The task of loads to different topical layers and their classes are settled based on specialists' perspective and site explicit circumstances. The drilling test and stratigraphic investigation are the most fundamental techniques for connecting the borehole's location and the depth of the materials to the groundwater resources (Jha et al. 2010). Numerous researchers have used a variety of methodologies, including decision tree model (Lee and Lee 2015), artificial neural network (Lee et al. 2017), frequency ratio (Guru et al. 2017; Al-Abadi et al. 2016), logistic regression mode (Pourtaghi and Pourghasemi 2014), random forest model (Naghbi et al. 2016), etc. These mostly focus on bivariate and multivariate statistical approaches, as well as sensitivity analysis and formulating assumptions before conducting an investigation (Thapa et al. 2017). A large portion of these methodologies depend on bivariate and multivariate measurable procedures with restrictions in making presumptions before examination and awareness of discoveries (Thapa et al. 2017). In this particular situation, the logical pecking order process (AHP) is regarded as a fundamental, simple, effective, and reliable approach (Machiwal et al. 2011; Ishizaka and Labib 2011), and

thus can be utilized for outlining groundwater expected zones. Many governments have initiated many projects, doing many researches to save the groundwater level ultimately. The central and other state governments of India have taken initiatives to regulate the program and management of the national groundwater resources.

Given the dynamic nature of groundwater, combining remote sensing (RS) data with geological data framework (GIS) information can be very beneficial in identifying groundwater likely zones (Agarwal and Garg 2016) that can be used to create valuable designs (Aluko and Igwe 2017). To delineate the groundwater potential zone, the logical progressive system methodology proposed by Saaty (1980) is combined with the RS-GIS technology. According to Sahoo et al. (2017), the AHP is a reliable tool for determining the groundwater potential zone (GWPZ). Groundwater potential zone identification using remote sensing (RS) data in geographic information systems (GIS) is obviously suitable (Agarwal and Garg 2016). The layers mean the various attributes which ultimately make the GWPZ are arbitrary. Various attribute layers have been used in this study, which are based on existing research works (Table 1). Combining GIS and AHP can be summed up as a cycle that shifts and combines topographical data and weighted location to recover information for independent movement (Malczewski 2006). The analytic hierarchy process (AHP) was found to be an effective tool for multi-criteria analysis (Saaty 2008; Hossein et al. 2016; Aneesh and Deka 2015; Gupta et al. 2018a, b).

The current article uses a coordinated RS and GIS methodology to display GWPZ in the Duars area (an area of India's Indo-Gangetic plain). This area has been identified as the Indian territory of West Bengal's most likely area for development by the Agro-Climatic Regional Planning Unit (Patra et al. 2016). The development of minor irrigation is coming through village irrigation. This comprehensive methodology of classification is supposed to guarantee protection of supportable spring improvement by sensible extraction of dynamic groundwater asset accessible in a specific zone. CGWB (2019) reported that India has over 249 m³ of groundwater. About half of Bengal gets their drinking water from underground. Groundwater also irrigates land for agriculture. It is a primary groundwater source in the eastern, southern and western parts of West Bengal. The high density of population, fast growing urbanization, agriculture-dependent people and extensive irrigation have created stress in the groundwater storage of West Bengal. The most important reason for groundwater overexploitation is agricultural irrigation that accounts for nearly 30% of withdrawal. Groundwater availability in West Bengal has been reported to be less than 20 BCM and resources used annually by the state are estimated at 25% that have been limited due to adverse

impact on the environment, sustainability and aquifer recharge process (Rudra et al. 2017). Many researchers revealed that groundwater resources in West Bengal are only one-fourth of its potential availability. In comparison, less work has been done in the field of agriculture and tea industry dependent on the alluvial-Duars landscape (Saha et al. 2010, 2021; Patra et al 2018; Biswas et al. 2020; Dey et al. 2021; Barua et al. 2021). West Bengal is one of the states in India with the lowest water availability, and its groundwater resources are under severe stress. Groundwater is directly or indirectly necessary for the daily survival of more than 90% of rural and 30% of urban populations (Patra et al. 2018). In the present research, a total of 12 parameters have been selected for estimating groundwater prospects in duars area of West Bengal. Also, to safeguard agricultural expansion with tea garden and urban area development, groundwater potentiality map is very much useful to manage it properly. The present research attempts to demarcate potential area of groundwater using MCDA-AHP and a GIS-based approach. The sustainable growth of agricultural regions and the long-term use of groundwater for irrigation, particularly in areas of agricultural predominance, depend on the management and mapping of groundwater resources in rural areas. Keeping the above view in mind, the present paper would address the following two objectives:

- (1) To delineate groundwater potential zones using AHP techniques during the period 2018–2019 to 2020–2021.
- (2) To validate the ROC between the output layer of potential zone and surveyed data.

Study area

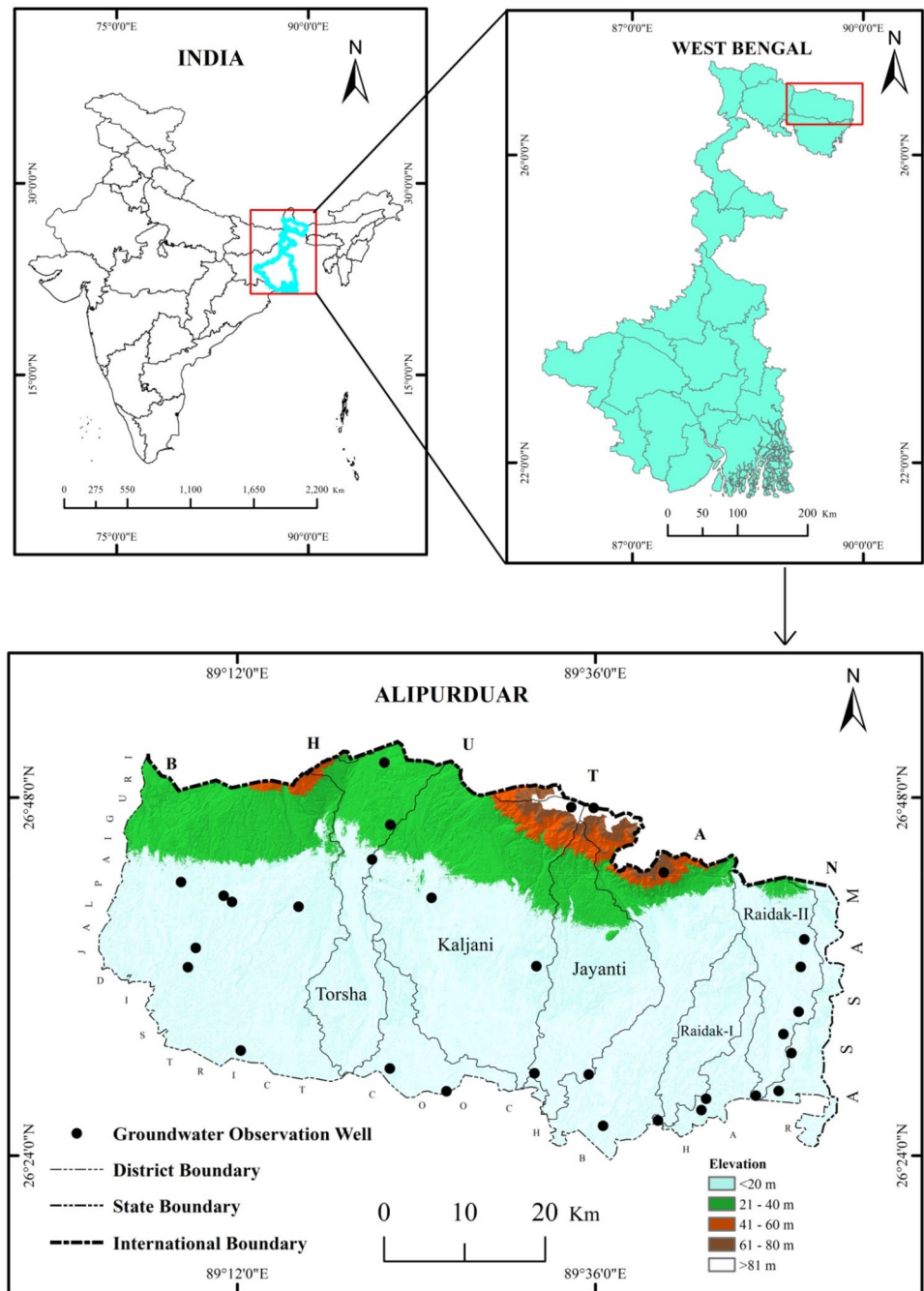
The Alipurduar district is located in the northwest of West Bengal, bordering Assam to the east and Bhutan to the north. The expansion of Alipurduar district (Fig. 1) is between 89°12'0"E and 89°36'0"E longitude and 26°24'0"N and 26°48'0"N latitude. It extends between the southern limit of Bhutan on the north and the Cooch Behar region toward the south; on the eastern side it connects to the western limit of Assam and on the western side lies the leftover piece of the Jalpaiguri area. There are six community development blocks, namely, Madarihat–Birpara (380.96 km²), Alipurduar-I (378.59 km²), Alipurduar-II (318.92 km²), Falakata (353.93 km²), Kalchini (711.61 km²), and Kumargram (517.68 km²) in the district. The complete geological space of the area is 2788 km². The environment of this locality is warm and wet. In summers, the temperature runs up to 38°C in May–June and in winter the temperature decreases up to 6°C in December–January. The normal precipitation of this region is 350 cm and the annual rainfall is about 3411 mm. The Ganga and Brahmaputra rivers deposited the majority

Table 1 Literature review for factors (theme) used to identify groundwater potential zones (GWPZ)

| Literature review | DEM | DD | NDWI | Aspect | RF | SL | NDVI | G | Soil texture | Pre-monsoon | Post-monsoon | LU/LC | GM | RR | SW | L/LD | LI | WTD |
|------------------------------------|-----|----|------|--------|----|----|------|---|--------------|-------------|--------------|-------|----|----|----|------|----|-----|
| Present Study | C | C | C | C | C | C | C | C | C | C | C | C | | | | | | |
| Murthy (2000) | | C | | C | C | C | | | C | | | C | C | | | | | |
| Jaiswal et al. (2003) | | C | | | C | C | | | C | | | C | C | | | | C | |
| Sikdar et al. (2004) | | C | | | | C | | C | | | | C | C | | | | | |
| Sener et al. (2005) | C | C | | | C | C | | | | | | C | C | | | | C | |
| Srivastava and Bhattacharya (2006) | | C | | | | C | | | C | | | C | C | | | | C | |
| Prasad et al. (2008) | | C | | | | C | | C | | | | C | C | | | | C | |
| Madrucci et al. (2008) | | | | | | C | | C | | | | C | C | | | | C | |
| Chowdhury et al. (2009) | | C | | | | C | | C | | | | C | C | C | | | | |
| Nagarajan and Singh (2009) | | C | | | | C | | | C | | | C | C | | | | | |
| Jha et al. (2010) | | C | | | | C | | | C | | | C | C | C | | | | |
| Chenini et al. (2010) | | C | | | | | | | C | | | C | C | | | | C | |
| Preeja et al. (2011) | | C | | | | | | C | | | | C | C | C | C | | | C |
| Machwal et al. (2011) | | | | | | | | | C | | | C | C | C | C | | | |
| Magesh et al. (2012) | C | C | | | | C | | | C | | | C | C | | | | | |
| Mukherjee et al. (2012) | C | C | | | | C | | | C | | | C | C | | | | | |
| Nag and Ghosh (2013) | | | | | | C | | | C | | | C | C | | | | | |
| Agarwal et al. (2013) | C | C | | | | C | | C | | | | C | C | | | | | C |
| Bagyaraj et al. (2013) | | C | | | | C | | C | | | | C | C | | | | | |
| Mahmoud et al. (2014) | | C | | | | C | | | C | | | C | C | | | | | |
| Zaidi et al. (2015) | | | | | | C | | C | | | | C | C | | | | | |
| Senanayake et al. (2016) | C | C | | | | C | | C | | | | C | C | | | | | C |
| Agarwal and Garg (2016) | C | C | | | | C | | C | | | | C | C | | | | | |
| Ibrahim-Bathis and Ahmed (2016) | | C | | | | C | | C | | | | C | C | C | C | | | |
| Jasrotia et al. (2016) | | C | | | | C | | C | | | | C | C | | | | | C |

DEM - digital elevation model, DD - drainage density, NDWI - normalized difference water index, Aspect, LU/LC - land use/land cover, RF - rainfall, SL - slope, NDVI - normalized difference vegetation index, G - geology, soil texture, pre-monsoon, post-monsoon, GM - geomorphology, RR - recharge rate, SW - surface water body, L/LD - lineament/lineament density, LI - lithology, WTD - water table depth

Fig. 1 Location map of Alipurduar district



of the alluvial sediments that make up the states’ subsurface. The unconsolidated formation forms potential aquifers in these piedmont zones of the Himalayas. Mainly, soils are shallow to moderately coarse loam soils, followed by deep to very deep clay loamy soils. The district has five major rivers.

The area is celebrated for timberland, untamed life, tea and wood. As per census of India 2011, total population of Alipurduar district is 1,491,250. Most of the people depend on agriculture practices and grow kharif and rabi crops in this region. Presently, there are many tea gardens adjacent to the forested fringe area and national highway.

Many tribal people living since long back in the area now work as tea garden workers. Despite the fact that the majority of the workforce is illiterate, they are increasingly urging their children to pursue education (Ansari and Sheereen 2016). In the district, area under settlements, agricultural fallow land, vegetation, bad-land topography, agricultural land and rivers is about 209.71 km², 525.76 km², 685.72 km², 659.17 km², 816.27 km² and 239.37 km², respectively. The net irrigation area is 87.7 (‘000 ha) and the gross is 234.30 km². Agricultural-dependent people use open well, bore well, and micro-irrigation method. The area has many

tea gardens and utilize the tube well water for irrigation. The district has no overexploited tehsils or blocks, but has five critical (Agricultural contingency report 2016) areas. In this belt, the majority of the aquifers are both semi-confined and unconfined. Pre-monsoon and post-monsoon periods saw a range of 1.05 to 19.72 m bgl in the depth of water observed by CGWB at 20 locations in the district (<http://cgwb.gov.in/>). The area is geographically very important to the north-east state of India and northern West Bengal. The rivers with their tributaries come down from Bhutan or adjacent to the Bhutan hills and flow down over this Duars (Alipurduar) area following the slope to south.

Material and methods

Preparation of thematic layer and satellite-based data

Twelve thematic maps were used to clarify the groundwater potential zone in the study region, viz., drainage density, slope, rainfall-monsoon and post-monsoon groundwater table depth, land use and land cover, geology, soil, elevation (digital elevation model), normalized differentiated wet index (NDWI), normalized differentiated vegetation index (NDVI), which were prepared using satellite-based imagery and related datasets. Satellite-based information (Table 2) was collected from USGS, Direct Imaging Self Filtering sensor (Landsat 8), which gave a goal of 30 m in the multispectral mode for use in the examination. Survey of India (SOI) geographical toposheet 1:50,000 scale was utilized for readiness of base guides. The Study of India geological guidelines were used to construct the SRTM and waste layer at a scale of 1:50,000. The seepage was refreshed with the (Aster Dem-30 m) satellite picture. The drainage network was superimposed with Aster DEM satellite image.

The guide portraying soils nearby on a 1:250,000 scale was arranged dependent on a dirt guide distributed by NBSS and LUP (<https://nbsslup.icar.gov.in/>), Administration of India. The slant map was created from Cutting edge Spaceborne Warm Outflow and Reflection Radiometer Computerized Rise Model (ASTER DEM-30 m Resolution). Rainfall data were collected from India Meteorological Department (<https://mausam.imd.gov.in/>) for 1 year (2021). The Landsat 8 (30 m) Operational Land Imager is used to create a supervised land use map, land cover map, and NDVI map. For ease of use, GIS data were geo-rectified and mapped to zone 45 of the Universal Transverse Mercator (Table 2).

The topographical guide was gathered from the Geographical Review of India and Legislature of India and filtered, redressed, and digitized in ArcGIS programming (version 10.8) to set up the land map. To separate possible zones, this load of topical layers was incorporated utilizing Arc Info GIS programming.

Pre-monsoon and post-monsoon groundwater depth maps were created by combining the annual and monthly data. The India-Water Resource Information System (WRIS) (<https://indiawris.gov.in/wris>), SWID (<http://wbwridd.gov.in/swid>) of the West Bengal government's data were used to monitor the groundwater levels. The data were both processed and shown on the appropriate map for future analysis. Throughout the course of this study, 30 observation wells were monitored monthly (2021–22) to validate the research work, and to obtain historical data, we made four observations every year in the months of April, August, November, and January between the years 2018 and 21. Inverse distance weighted deterministic interpolation was used to generate yearly the average pre- and post-monsoon groundwater depth maps (IDW). Groundwater depth maps for the pre- and post-monsoon periods were created using IDW interpolation. The simplest interpolation method is this one. In this case, a weighting function determines the weight.

Table 2 Brief description of datasets used in this study

| Attribute | Time of the dataset | Sources | Acquisition date |
|-----------------------------------------------------------------------------|---------------------|-------------------------------------------------------------------------------------------------------------------|--------------------------|
| LANDSAT 8 (spatial resolution 30 m) (LC08_L1TP_138042_20200406_20200410_01) | 04.06.2020 | USGS earth explorer | 21.12.2021 |
| ASTER DEM (spatial resolution 30 m) (n26_e089_3arc_v2.tif) | 2021 | USGS earth explorer | 21.12.2021 |
| Soil texture map | 2021 | NBSS&LUP | 01.02.2022 |
| Rainfall data | 2021 | India Meteorological Department (IMD) | 11.02.2022 |
| Geology | 28.10.2021 | Bhuvan | 21.12.2021 |
| Groundwater data | 2018–2021 | Central Ground Water Board (CGWB), India and The State Water Investigation Directorate, Government of West Bengal | 11.04.2022 05.08.2022 |

Table 3 Pairwise comparison matrix of GWPZ

| Themes | Assigned weight | Elevation (m) | Drainage density (km ²) | NDWI | Aspect | Rainfall (mm) | Slope(degree) | NDVI | Geology | Soil Texture | Pre-Monsoon groundwater depth (m bgl) | Post-Monsoon groundwater (m bgl) | LULC | Geometric mean | New weight |
|------------------|-----------------|---------------|-------------------------------------|------|--------|---------------|---------------|------|---------|--------------|---------------------------------------|----------------------------------|------|----------------|------------|
| Elevation | 9 | 1.00 | 0.90 | 1.00 | 1.13 | 1.29 | 1.50 | 1.80 | 1.80 | 3.00 | 4.50 | 4.50 | 1.29 | 1.97 | 0.12 |
| Drainage density | 10 | 1.11 | 1.00 | 1.11 | 1.25 | 1.43 | 1.67 | 2.00 | 2.00 | 3.33 | 5.00 | 5.00 | 1.43 | 2.19 | 0.14 |
| NDWI | 9 | 1.00 | 0.90 | 1.00 | 1.13 | 1.29 | 1.50 | 1.80 | 1.80 | 3.00 | 4.50 | 4.50 | 1.29 | 1.97 | 0.12 |
| Aspect | 8 | 0.89 | 0.80 | 0.89 | 1.00 | 1.14 | 1.33 | 1.60 | 1.60 | 2.67 | 4.00 | 4.00 | 1.14 | 1.76 | 0.11 |
| Rainfall | 7 | 0.78 | 0.70 | 0.78 | 0.88 | 1.00 | 1.17 | 1.40 | 1.40 | 2.33 | 3.50 | 3.50 | 1.00 | 1.54 | 0.08 |
| Slope | 6 | 0.67 | 0.60 | 0.67 | 0.75 | 0.86 | 1.00 | 1.20 | 1.20 | 2.00 | 3.00 | 3.00 | 0.86 | 1.32 | 0.08 |
| NDVI | 5 | 0.56 | 0.50 | 0.56 | 0.63 | 0.71 | 0.83 | 1.00 | 1.00 | 1.67 | 2.50 | 2.50 | 0.71 | 1.10 | 0.07 |
| Geology | 5 | 0.56 | 0.50 | 0.56 | 0.63 | 0.71 | 0.83 | 1.00 | 1.00 | 1.67 | 2.50 | 2.50 | 0.71 | 1.10 | 0.07 |
| Soil texture | 3 | 0.33 | 0.30 | 0.33 | 0.38 | 0.43 | 0.50 | 0.60 | 0.60 | 1.00 | 1.50 | 1.50 | 0.43 | 0.66 | 0.04 |
| Pre-monsoon | 2 | 0.22 | 0.20 | 0.22 | 0.25 | 0.29 | 0.33 | 0.40 | 0.40 | 0.67 | 1.00 | 1.00 | 0.29 | 0.44 | 0.03 |
| Post-monsoon | 2 | 0.22 | 0.20 | 0.22 | 0.25 | 0.29 | 0.33 | 0.40 | 0.40 | 0.67 | 1.00 | 1.00 | 0.29 | 0.44 | 0.03 |
| LULC | 7 | 0.78 | 0.70 | 0.78 | 0.88 | 1.00 | 1.17 | 1.40 | 1.40 | 2.33 | 3.50 | 3.50 | 1.00 | 1.54 | 0.10 |

Table 4 Normalized matrix of GWPZ

| Themes | Elevation (m) | Drainage density (km ²) | NDWI | Aspect (mm) | Rainfall (mm) | Slope (degree) | NDVI | Geology | Soil texture | Pre-Monsoon groundwater depth (m bgl) | Post-Monsoon groundwater depth (m bgl) | LULC | Weighted sum | Row average | λ |
|------------------|---------------|-------------------------------------|------|-------------|---------------|----------------|------|---------|--------------|---------------------------------------|----------------------------------------|------|--------------|-------------|-----------|
| Elevation | 0.12 | 0.12 | 0.12 | 0.12 | 0.12 | 0.12 | 0.12 | 0.12 | 0.12 | 0.12 | 0.12 | 0.12 | 1.48 | 0.12 | 12 |
| Drainage density | 0.14 | 0.14 | 0.14 | 0.14 | 0.14 | 0.14 | 0.14 | 0.14 | 0.14 | 0.14 | 0.14 | 0.14 | 1.64 | 0.14 | 12 |
| NDWI | 0.12 | 0.12 | 0.12 | 0.12 | 0.12 | 0.12 | 0.12 | 0.12 | 0.12 | 0.12 | 0.12 | 0.12 | 1.48 | 0.12 | 12 |
| Aspect | 0.11 | 0.11 | 0.11 | 0.11 | 0.11 | 0.11 | 0.11 | 0.11 | 0.11 | 0.11 | 0.11 | 0.11 | 1.32 | 0.11 | 12 |
| Rainfall | 0.10 | 0.10 | 0.10 | 0.10 | 0.10 | 0.10 | 0.10 | 0.10 | 0.10 | 0.10 | 0.10 | 0.10 | 1.15 | 0.10 | 12 |
| Slope | 0.08 | 0.08 | 0.08 | 0.08 | 0.08 | 0.08 | 0.08 | 0.08 | 0.08 | 0.08 | 0.08 | 0.08 | 0.99 | 0.08 | 12 |
| NDVI | 0.07 | 0.07 | 0.07 | 0.07 | 0.07 | 0.07 | 0.07 | 0.07 | 0.07 | 0.07 | 0.07 | 0.07 | 0.82 | 0.07 | 12 |
| Geology | 0.07 | 0.07 | 0.07 | 0.07 | 0.07 | 0.07 | 0.07 | 0.07 | 0.07 | 0.07 | 0.07 | 0.07 | 0.82 | 0.07 | 12 |
| Soil texture | 0.04 | 0.04 | 0.04 | 0.04 | 0.04 | 0.04 | 0.04 | 0.04 | 0.04 | 0.04 | 0.04 | 0.04 | 0.49 | 0.04 | 12 |
| Pre-monsoon | 0.03 | 0.03 | 0.03 | 0.03 | 0.03 | 0.03 | 0.03 | 0.03 | 0.03 | 0.03 | 0.03 | 0.03 | 0.33 | 0.03 | 12 |
| Post-monsoon | 0.03 | 0.03 | 0.03 | 0.03 | 0.03 | 0.03 | 0.03 | 0.03 | 0.03 | 0.03 | 0.03 | 0.03 | 0.33 | 0.03 | 12 |
| LULC | 0.10 | 0.10 | 0.10 | 0.10 | 0.10 | 0.10 | 0.10 | 0.10 | 0.10 | 0.10 | 0.10 | 0.10 | 1.15 | 0.10 | 12 |

Table 5 Saaty’ (1980) ratio index for different values of N

| N | 1 | 2 | 3 | 4 | 5 | 6 | 7 | 8 | 9 | 10 | 11 | 12 | N=number of parameters |
|----|------|------|------|-----|------|------|------|------|------|------|------|------|------------------------|
| RI | 0.00 | 0.00 | 0.58 | 0.9 | 1.12 | 1.24 | 1.32 | 1.41 | 1.45 | 1.49 | 1.51 | 1.49 | RI=random indices |

Deriving the weights using the analytic hierarchy process (AHP)

For groundwater inquiry and good groundwater potential mapping, remote sensing and GIS are helpful tools. Many scientists and academics have used the GIS applications and the remote sensing techniques to map out groundwater supplies and potential zones. Multi-criteria decision-making (MCDM) based on GIS emerges is one of the most effective techniques for managing and planning for space. The analytical hierarchy process (AHP) is among the most widely used techniques for obtaining spatial plans, resource allocation, etc. A new method for mapping groundwater potential zones has been adopted, although only a small number of studies have used it (Patra et al. 2018). These studies explicitly map potential zones and integrate multi-criteria analysis utilizing weighted aggregation method coupled with GIS tools.

Twelve parameters were used in the current investigation, and weights were assigned based on the AHP technique (Table 3). Greater weight was given in accordance with its potential for groundwater, and vice versa. Further, pairwise comparison matrix using Saaty’s 12-point weight scale was calculated and applied to the following methods.

1. Step 1. Establishment of judgment matrices (P) by pairwise comparison:

$$P = \begin{bmatrix} p_{11} & p_{12} & \dots & p_{1n} \\ p_{21} & p_{22} & \dots & p_{2n} \\ \vdots & \vdots & \dots & \vdots \\ p_{1n} & p_{2n} & \dots & p_{nn} \end{bmatrix}, \tag{1}$$

where p_n denotes the nth indicator element with p_{nn} is the judgment matrix element.

2. Step 2. Calculation of normalized weight: where the geometric mean of the 1 row of the judgment matrices is calculated as

$$W_n = \left\{ \frac{GM_n}{\sum_{n=1}^{N_f} GM_n} \right\}, \tag{2}$$

$$GM_n = \sqrt[N_f]{P_{1n} \dots P_{nn} N_f}. \tag{3}$$

3. Step 3. Calculating a consistency ratio (CR) to evaluate the consistency of decisions:

$$CR = \frac{CI}{RCI}. \tag{4}$$

Consistency Index (CI) is denoted as follows :

$$CI = \frac{\lambda_{max} - N_f}{N_f - 1}, \tag{5}$$

where λ_{max} is the eigen value of the judgement matrix and is calculated as

$$\lambda_{max} = \sum_{n=1}^{N_f} \frac{(PW)_n}{N_f W_n}. \tag{6}$$

Assessing the matrix consistency

Primarily chosen classes are reclassified and assigned accordingly. A specific criterion of the study region is constructed as sub-criteria and ranges specify the maximum and minimum variances (characteristics). Typically, different levels are re-categorized, according to which they are ranked. The creation aims to highlight the strongest aspects of a certain topic of study. It is based on the authors’ own experiences and literary analysis. The final step involves creating prospective groundwater index maps on the GIS platform using weighted linear combinations of individual standard layers. Here, potential indicators of groundwater have been calculated (Sahoo et al. 2017). The steps listed below are followed to compute the consistency ratio (CR): (1) principal eigen value (λ) is computed using the eigen vector approach (Table 4). The equation described below was used to determine the consistency index (CI) (Saaty 1990; Arulbalaji et al. 2019).

The total work process of approach is given below:
 $\lambda_{max} = 144/12 = 12.$

4. **Step-1.** $C.I = (\lambda_{max} - n) / (n - 1),$

where λ_{max} = the principal eigenvalue and n = the number of parameters used in the analysis.

5. **Step-2.** Consistency index (CI) is denoted as follows:

$$C.I = (12 - 12) / (12 - 1) = 0.$$

Table 6 Assigned and normalized weights of different features of 12 thematic layers for groundwater potential zone

| SL no. | Factor | Weight | Indicator level | Sub-feature class | Area in % | Normalized weight |
|--------|------------------|--------|-----------------|---------------------------------------------------------------------|-----------|-------------------|
| 1 | Elevation | 9 | S ₁ | < 20 | 96.23 | 0.28 |
| | | | S ₂ | 21–40 m | 01.94 | 0.25 |
| | | | S ₃ | 41–60 m | 01.02 | 0.19 |
| | | | S ₄ | 61–80 m | 00.47 | 0.17 |
| | | | S ₅ | > 81 m | 00.34 | 0.11 |
| 2 | Drainage density | 10 | S ₆ | < 0.20 km/km ² | 17.44 | 0.29 |
| | | | S ₇ | 0.21–0.40 km/km ² | 25.79 | 0.23 |
| | | | S ₈ | 0.41–0.60 km/km ² | 26.56 | 0.20 |
| | | | S ₉ | 0.61–0.80 km/km ² | 21.02 | 0.19 |
| | | | S ₁₀ | > 0.81 km/km ² | 09.19 | 0.09 |
| 3 | NDWI | 9 | S ₁₁ | (–) 0.23–0.012 | 12.32 | 0.10 |
| | | | S ₁₂ | 0.013–0.072 | 24.34 | 0.15 |
| | | | S ₁₃ | 0.073–0.13 | 29.32 | 0.20 |
| | | | S ₁₄ | 0.14–0.18 | 27.66 | 0.30 |
| | | | S ₁₅ | 0.19–0.39 | 06.36 | 0.25 |
| 4 | Aspect | 8 | S ₁₆ | N | 19.84 | 0.15 |
| | | | S ₁₇ | NE | 12.04 | 0.10 |
| | | | S ₁₈ | E & NW | 19.33 | 0.15 |
| | | | S ₁₉ | SE & W | 23.99 | 0.40 |
| | | | S ₂₀ | S | 12.53 | 0.10 |
| | | | S ₂₁ | SW | 12.27 | 0.10 |
| 5 | Rainfall | 7 | S ₃₀ | < 701 mm | 46.50 | 0.34 |
| | | | S ₃₁ | 702–1401 mm | 12.68 | 0.22 |
| | | | S ₃₂ | 1402–2101 mm | 26.64 | 0.29 |
| | | | S ₃₃ | 2102–2801 mm | 09.18 | 0.10 |
| | | | S ₃₄ | > 2802 mm | 05.00 | 0.05 |
| 6 | Slope | 6 | S ₃₅ | < 3 ⁰ | 62.53 | 0.33 |
| | | | S ₃₆ | 4–6 ⁰ | 26.95 | 0.28 |
| | | | S ₃₇ | 7 ⁰ –12 ⁰ | 06.16 | 0.19 |
| | | | S ₃₈ | 13 ⁰ –24 ⁰ | 02.91 | 0.12 |
| | | | S ₃₉ | > 25 ⁰ | 01.45 | 0.08 |
| 7 | NDVI | 5 | S ₄₀ | (–) 0.05–0.15 | 06.04 | 0.14 |
| | | | S ₄₁ | 0.16–0.22 | 12.47 | 0.17 |
| | | | S ₄₂ | 0.23–0.28 | 59.21 | 0.43 |
| | | | S ₄₃ | 0.29–0.33 | 22.28 | 0.26 |
| 8 | Geology | 5 | S ₄₄ | Undivided Paleozoic | 00.12 | 0.34 |
| | | | S ₄₅ | Pliocene Pleistocene | 01.18 | 0.28 |
| | | | S ₄₆ | Proterozoic | 03.42 | 0.21 |
| | | | S ₄₇ | Quaternary | 95.28 | 0.17 |
| 9 | Soli texture | 3 | S ₄₈ | Coarse loamy, umbric dystrochrepts | 09.03 | 0.16 |
| | | | S ₄₉ | Fine loamy, aeric haplaquepts, coarse loamy, typic ustorthents | 01.34 | 0.13 |
| | | | S ₅₀ | Fine loamy, fluventic eutrochrepts, coarse loamy, aquic udifluvents | 18.82 | 0.24 |
| | | | S ₅₁ | Coarse loamy, aquic ustifluvents, fine fluvaquents | 01.26 | 0.30 |
| | | | S ₅₂ | Coarse loamy, typic haplaquents, coarse loamy, typic fluvaquents | 69.55 | 0.17 |

Table 6 (continued)

| SL no. | Factor | Weight | Indicator level | Sub-feature class | Area in % | Normalized weight |
|--------|--------------------------------|--------|-----------------|--------------------------|-----------|-------------------|
| 10 | Pre-monsoon groundwater depth | 2 | S ₅₃ | 0.61–2.90 m bgl | 66.78 | 0.28 |
| | | | S ₅₄ | 3.00–5.10 m bgl | 18.83 | 0.20 |
| | | | S ₅₅ | 5.20–7.40 m bgl | 07.34 | 0.18 |
| | | | S ₅₆ | 7.50–9.60 m bgl | 04.86 | 0.20 |
| | | | S ₅₇ | 9.70–12.00 m bgl | 02.19 | 0.14 |
| 11 | Post-monsoon groundwater depth | 2 | S ₅₈ | 0.88–4.30 m bgl | 82.19 | 0.29 |
| | | | S ₅₉ | 4.40–7.60 m bgl | 10.12 | 0.25 |
| | | | S ₆₀ | 7.70–11.00 m bgl | 04.16 | 0.19 |
| | | | S ₆₁ | 12.00–14.00 m bgl | 02.29 | 0.16 |
| | | | S ₆₂ | 15.00–18.00 m bgl | 01.24 | 0.11 |
| 12 | Land use and land cover (LULC) | 7 | S ₂₂ | Tea garden | 12.39 | 0.14 |
| | | | S ₂₃ | Sparse forest | 02.67 | 0.13 |
| | | | S ₂₄ | Dense forest | 21.18 | 0.13 |
| | | | S ₂₅ | Cultivated land | 28.99 | 0.16 |
| | | | S ₂₆ | Settlement | 10.68 | 0.14 |
| | | | S ₂₇ | Water bodies | 09.62 | 0.17 |
| | | | S ₂₈ | Barren land | 03.19 | 0.05 |
| | | | S ₂₉ | Agricultural fallow land | 11.28 | 0.08 |

The ratio of CI to RCI is known as the consistency ratio (CR). (where the consistency index (CI) and random consistency index (RCI) are both used), whose value was determined using the Saaty’s standard (Saaty 1990) (Table 5).

6. **Step-3.** The consistency ratio (CI) is denoted as follows:

$$CR = CI/RCI.$$

$$CR = 0/1.49 = 0.$$

The delineation of groundwater potential zones by weighted overlay method

On the basis of the groundwater potential index (GPI), which is derived utilizing the following formula, the field's groundwater potential zone (GWPZ) was created by integrating eight relevant thematic levels into one layer (Shekhar and Pandey 2015; Das et al. 2018). The method is used to illustrate GWPZ by combining different techniques of RS, GIS and AHP as shown to separate groundwater likely zones (Fig. 2). After analyzing the interactions of various boundaries planned in the local GIS climate, all of the layers were spatially overlapped for a groundwater assets map. Groundwater potential zones are managed based on non-dimensional imaging. The indexing

of possible groundwater areas in an area is useful (Bonilla Valverde et al. 2016; Jha et al. 2010).

The weightages to every parameter has been given by following the Saaty’s scale of relative significance cost (Saaty 1990 and Arulbalaji et al. 2019). In addition, the weights are assigned to such theme layer on the basis of their significance for the possibility of groundwater recharge while taking into account literature review, field research, and observation. Accordingly, 12 thematic layers were compared with different criteria in a pairwise comparison matrix. Thematic layer subclasses were reclassified for use in the GIS platform's weighting system.

According to Shekhar and Pandey (2015), the groundwater potential index (GWPI), which expresses GWPZs in a given area, is a value without units (Das et al. 2018).

$$GWPI = \sum_{w=1}^m \sum_{j=1}^n (W_j \times X_i) \tag{6}$$

$$GWPI = EL_w EL_r + DD_w DD_r + NDWI_w NDWI_r$$

$$+ A_w A_r + R_w R_r + SL_w SL_r + NDVI_w NDVI_r$$

$$+ G_w G_r + ST_w ST_r + PR_w PR_r$$

$$+ PO_w PO_r + LU_w LU_r,$$

where EL stands for elevation, DD for drainage density, NDWI for normalized difference water index, A for aspect,

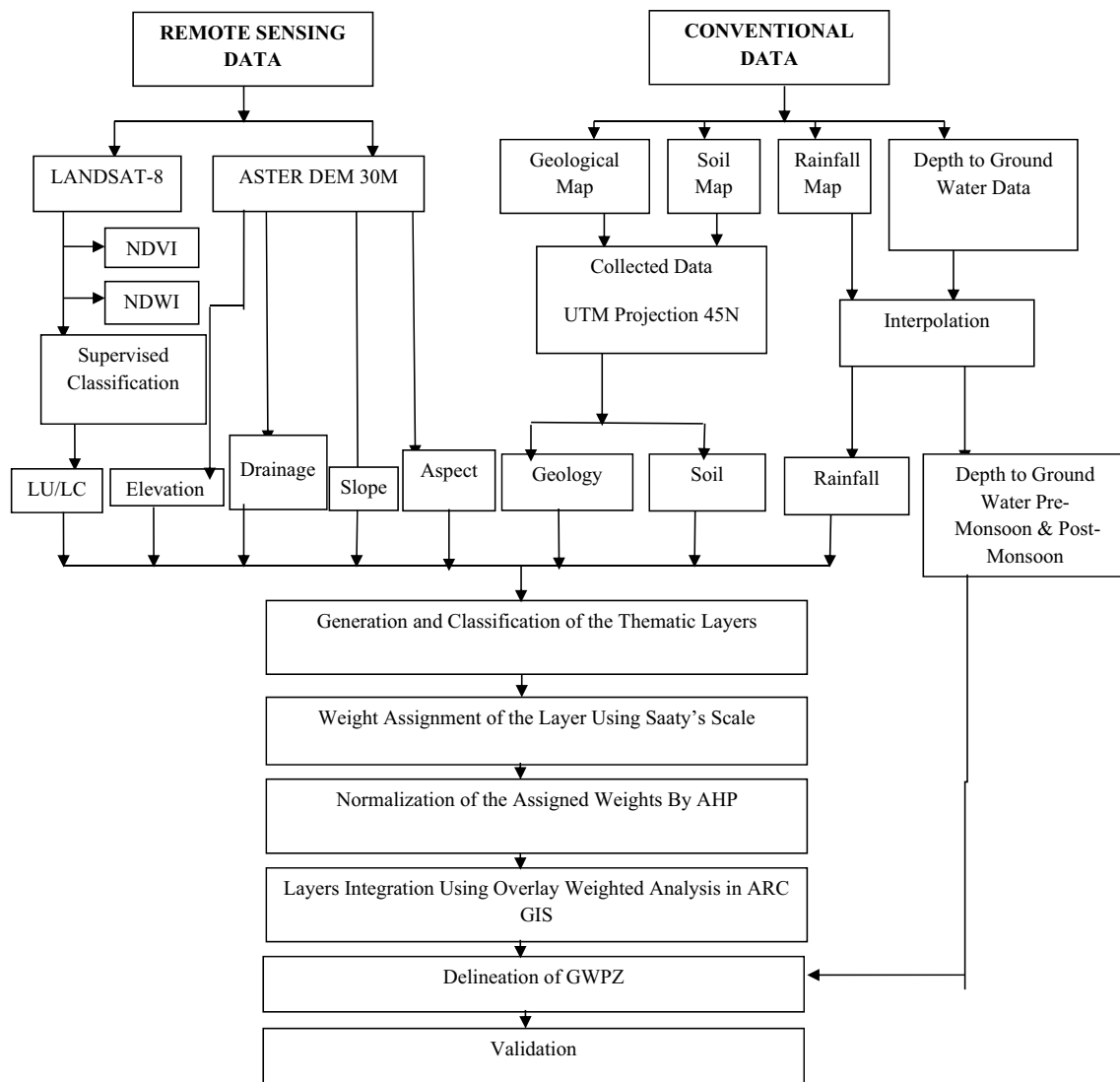


Fig. 2 Flowchart for the identification of groundwater potential zones in the study area

R for rainfall, SL for slope, NDVI for normalized difference vegetation index, G for geology, ST for soil texture, PR for pre-monsoon, PO for post-monsoon, and LU for land use/land cover. The letters "w" and "r" stand for the weight of a thematic layer and the ranking of subclasses within each layer, respectively.

Validation

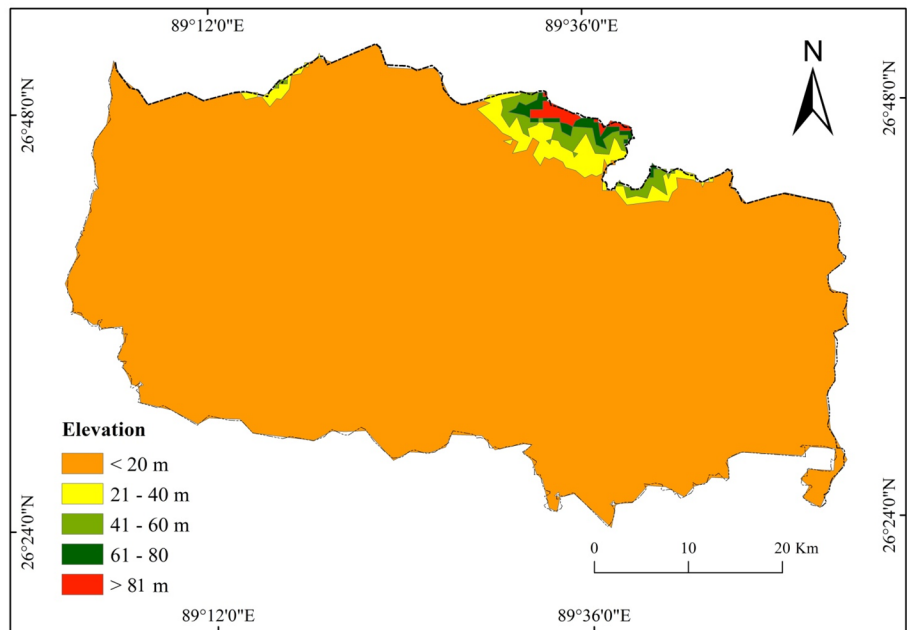
The monitored well (30 observation wells, 2021–2022) data were further studied to validate the research work. The validation method first starts with the final output of GWPZ and validates with ultimately collected well data. An important ROC using SPSS Software is used for this. The receiver operating characteristic curve (ROC curve) is a graph that displays how well a classification model performs across

all categorization levels. Two parameters are plotted on this curve: 1. true positive; 2. false positives. It is a graphical plot to diagnose the binary classifiers.

Results and discussion

Alipurduar district's several groundwater potential zones are identified by 12 (physical and man-made) different influencing elements, including elevation, drainage density and sub-drainage density, NDWI, aspect, rainfall, slope, NDVI, geology, soil texture, pre-monsoon groundwater depth, post-monsoon groundwater depth and land use and land cover. The physical and man-made elements, both influence the groundwater in reality. Based on the findings of this investigation, a thorough explanation is provided below. The necessary weights were

Fig. 3 Elevation map of the study area



applied to each layer in preparation for the overlay process after each layer's influence on the others and on itself was determined. The weight and the influence (Table 6) contains a list of the assignments for each tier.

Elevation

The review region's elevation map plainly reflects the landscape's roughness, which is a key factor in identifying the groundwater potential. The ground surface undulations available for depression storage are represented by the elevation of the study region (Saranya and Saravanan 2020). Lower height sections (plain regions) will typically store water for longer, allowing for more notable penetration of re-energized water. A lot of overflows and a more modest measure of invasion are related to regions with steep rise (Godebo 2005). ASTER DEM was used to create the elevation map (Fig. 3), which is essential for mapping the groundwater potential zone. The area's height varies from 93 m and was broken down into five classifications (Table 6). The water runoff from higher elevations accumulates in lower elevation areas and vice versa, low elevation indicates a rich groundwater potential zone. The elevation map has shown that about 96.23% of the area has very strong groundwater potential, whereas only 1.94 %, 1.02%, 0.47% and 0.34% area has good, moderate, low and very low groundwater potential, respectively. Lower the elevation, the more will be the groundwater recharge and vice-versa. The areas having less 20 m elevation are inducing greater infiltration, which recharges the groundwater. On the opposite side, area with elevation more than 80 m is rocky and having

immature soil, which is not suitable for groundwater recharge. The lower homogenous plain represents the old perennial and sluggish river flowing from Bhutan hill to south of the district. Also, the presence of sedimentary deposit permits more recharge to groundwater. Area which has less than 20 m (more than 80 m) elevation is assigned higher (lower) weightage.

Drainage density

Permeability, which controls the amount and rate of infiltration, is inversely related to drainage density (Ibrahim-Bathis and Ahmed 2016). When evaluating the groundwater zone, drainage density, an upgraded form of permeability, must be taken into account. To construct the drainage density map, the research area's drainage map is used. Low drainage density locations received higher ranks, whereas high drainage density areas received lower rankings. Compared to a location with a high drainage density, a low drainage density region results in higher infiltration and favorable groundwater potential zones (Bhunia. 2020; Barua et al. 2021; Senapati and Das 2021). Five categories were used for drainage density values. The drainage density (km/km²) of the research area was classified into five classes (Fig. 4), indicating very poor (<0.2km²), poor (0.21–0.40 km²), moderate (0.41–0.60 km²), good (0.61–0.80 km²) and very high (>0.80 km²). More weight allocation for low waste thickness and less weight distribution for high seepage thickness are used to identify potential groundwater zonation (Shekhar and Pandey 2015). The tributaries and main rivers of Alipurduar district have greater influence on

recharging the groundwater itself. The district shows higher ranks of drainage density. The rivers follow the slope, moving to the southern district of West Bengal. So, the flow of rivers has an important role in affecting the groundwater level and potentiality. 9.19% ($< 0.2 \text{ km}^2$) of the drainage density clearly depicts groundwater potential to be very high, 21.02% ($0.21\text{--}0.40 \text{ km}^2$) high, 26.56% ($0.41\text{--}0.60 \text{ km}^2$) moderate, 25.79% ($0.61\text{--}0.80 \text{ km}^2$) low, and 17.44% ($> 0.80 \text{ km}^2$) very low (Table 6).

Water levels of different rivers (drainage density)

During the rainy season, the irrigation department serves as the central hub for measuring water level status and communicating it to other departments that may be affected. In general, records are taken every 3 h, but in times of urgency, hourly statistics are gathered for each of the five main rivers. The following describes the aforementioned levels of all significant rivers which directly affect the groundwater level and potentiality in the research area. From west to east, there are several south flowing rivers which are perennial in nature, determining the water level in the district.

Torsa River

Torsa begins from Tibet, northern part of Bhutan and flows into the area through Phuntsholing, a city of Bhutan. The center course of this stream moves through Alipurduar area and finally converges with the Brahmaputra waterway in Bangladesh by means of Coochbehar. The complete length of the stream is 122 km with a catchment space of around 4530 km^2 . In Alipurduar, the bowl region is 252.6 km^2 . The catchment (Fig. 4A) is too restricted to even consider aggregating different feeders, which uncovers that it is anything but a solitary stream channel.

Jayanti Gadadhar

Jayanti is a small river flowing through Buxa forest area. This river originates in Bhutan and flows through Alipurduar district (Fig. 4B). This river remains dry almost throughout the year, and clear and cool water flows during the monsoons. The river Gadadhar is a tributary of Torsa river.

Raidak-I

After beginning in Bhutan, the stream travels through Bhutanghat to Alipurduar where it splits into two halves, known as Raidak-I and Raidak-II. Raidak-I (Fig. 4C) finally reaches

Bangladesh's Brahmaputra River, whereas Raidak-II meets the stream Sankosh at Baxirhat. This stream's catchment area is 268.17 sq km , or about half of the entire bowl region. This river basin's topography varies greatly from location to location, which makes the river risky for flash floods during the rainy season.

Raidak-II

This river is regarded as a tributary of the nearby Bhutanghat-bifurcated Raidak stream (Fig. 4D), which immediately passes through Kumargaram Block. At Baxirhat, it finally joins the Sankosh River, and the combined stream then flows into Bangladesh and joins the Brahmaputra. This stream's total catchment area is 184.38 square kilometers.

Kaljani

The rivers Pana and Basra from Bhutan enter the Alipurduar district after their rise and flow as a unit. Later it joins a river called Dima near the Alipurduar district and flows through the Alipurduar district as Kaljani river (known as life line of the Alipurduar district) (Fig. 4E). Kaljani river has also changed its course many times. Within this river basin, the topography differs greatly, which intensifies flash floods. With a catchment area of 664.8 square kilometers, this river basin is the largest in the Alipurduar district.

Normalized difference water index (NDWI)

To distinguish open water features and make them more visible in remotely sensed digital pictures, a new technique called the normalized difference water index (NDWI) has been created. The NDWI utilizes reflected close to infrared emission and apparent green light to upgrade the incidence of such highlights while dispensing with the presence of soil and earthly vegetation highlights. When using this NDWI formulation, an image is created in which the positive data values are often open water regions and the negative data values are typically non-water features (such as terrestrial vegetation and cover types with a predominance of bare soil) (Singh et al. 2017). The local scale for NDWI is -1 to $+1$, just like for NDVI. $\text{NDWI} = (\text{GREEN} - \text{NIR}) / (\text{GREEN} + \text{NIR})$ (Mcfeeters 1996) Five courses were established for NDWI (Fig. 5). NDWI is groped into five classes, such as very low (-0.23 to -0.012), low (-0.13 to 0.072), moderate (0.072 to 0.13), high (0.14 to 0.18) and very high (0.19 to 0.39). It has been found that about 12.32%, 24.34%, 29.32% areas have excellent, great and moderate groundwater potential, respectively. Whereas, about 27.66% and

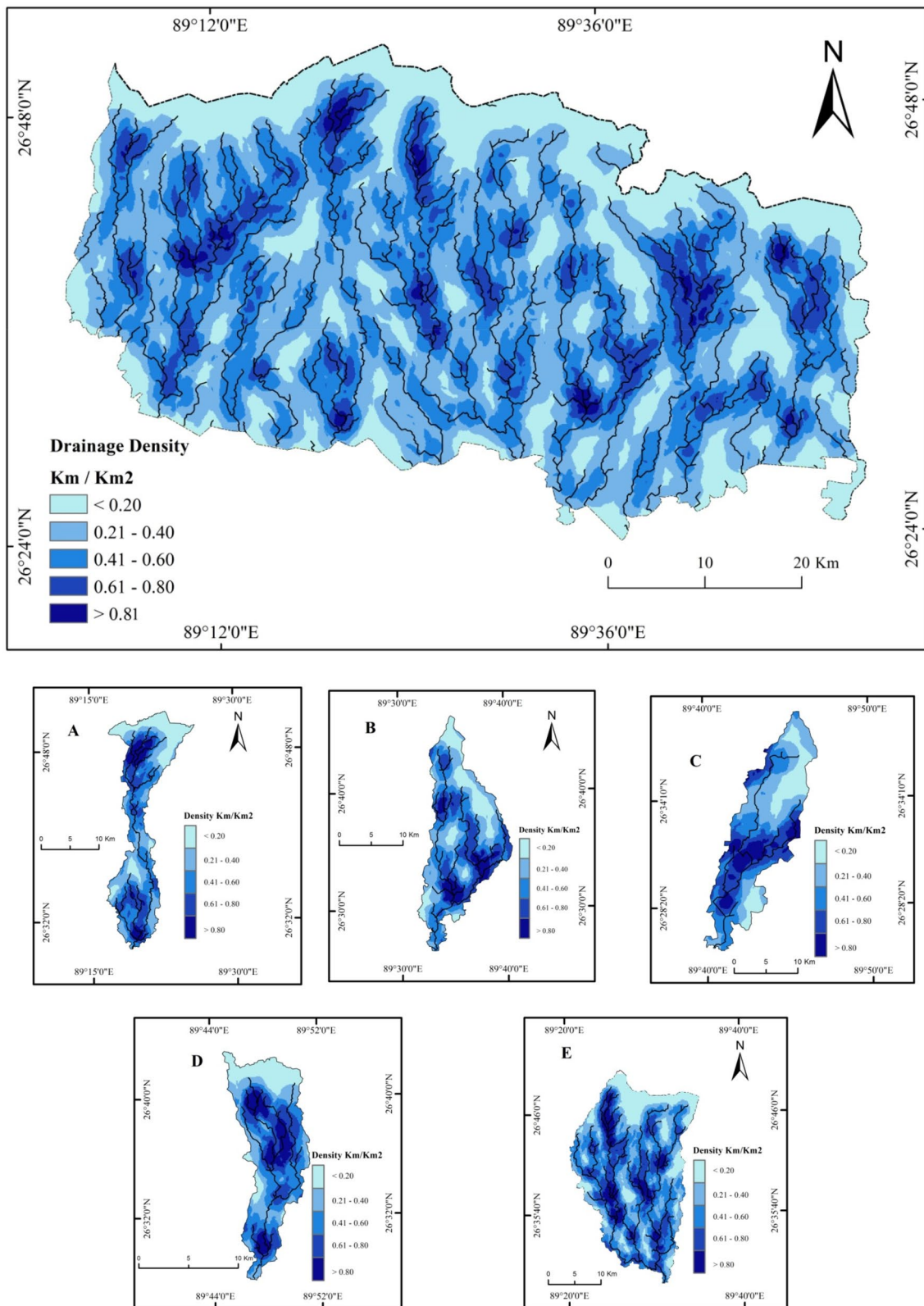
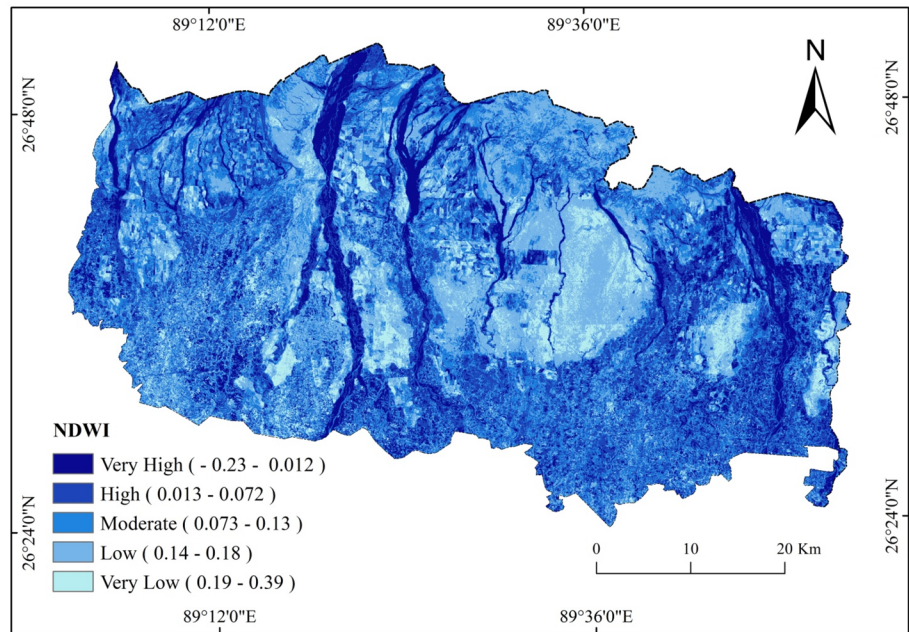


Fig. 4 Drainage density over Alipurduar district and different sub-basins. **A** Torsha, **B** Jayanti Gadadhar, **C** Raidak-I, **D** Raidak-II, **E** Kaljani

Fig. 5 NDWI pattern in the study area



6.36% areas have low to extremely low groundwater potential respectively. High weightage is given to very high NDWI class and low weightage (Table 6) is given to very low NDWI class.

Aspect

Aspect shows the direction of the maximum rate of value change from one cell to its neighbors, which is downward (Singh et al. 2017). The direction of the slope can be compared to aspect. Temperature can be significantly impacted by the aspect. This is due to the fact that aspect changes the angle at which the sun's rays strike the ground, which in turn affects how concentrated those rays are when they strike the ground. The compass course that a geographical incline faces is generally estimated in degrees from the north. Angle can impact temperature. This is on the grounds that perspective influences the point of the sun beams when they interact with the ground, and subsequently influences the convergence of the sun's beams hitting the earth. Viewpoint map was set up from ASTER DEM (Table 2). North-facing slopes had a high weighting since the effect of sunlight is quite low, while south-facing slopes received a very low weighting due to the angle of sunlight and time. Mid-winter light exposure on north-facing slopes is very low, especially in the Northern Hemisphere. Conversely, south-facing slopes have substantially higher temperatures than north-facing slopes. The prepared map aspect guide (Fig. 6) states that 19.84% region has generally excellent, 12.04% great, 19.33% moderate, 12.53% 23.99% moderate low, 12.53% low and 12.27% very low groundwater potential.

Rainfall

Another important factor that significantly affects groundwater potentiality and serves as a major source of groundwater recharge is rainfall, which is a component of the hydrological cycle (Abijith et al. 2020). Since maximal rainfall is related to a high rate of infiltration, the intensity and length of rainfall directly impact the rate of groundwater recharging. Additionally, the amount of rainfall permits the identification of a balance between subsurface groundwater recharge and discharge and is proportionally related to the renewal of groundwater capacity (Moges et al. 2019). Alipurduar is 49 m above mean sea level and close to Bhutan hill. In Alipurduar, the environment is warm and mild. In winter, there is significantly less precipitation than in summer. This environment is viewed as Cwa as indicated by the Koppen–Geiger environment arrangement. The precipitation here is around 3411 mm–134.3 mm each year. The driest month is November. There is 5 mm of precipitation in November. With a normal of 848 mm–33.4 mm, the most precipitation is in July. Alipurduar is a heavy precipitation region in West Bengal. Rainstorm cloud enters from the south and tends to go toward north and produce immense precipitation over this region due to obstruction of mountain range. Low long-term precipitation affects low penetration and excessive surface runoff. The average annual rainfall also affects groundwater recharge. Higher rainfall is associated with a higher groundwater potential, while lower rainfall is associated with a lower groundwater potential. By using an IDW interpolation method of rainfall data for the selected research area, the rainfall map of the thematic layer is produced (Fig. 7). The map shows classification into five zones, namely, < 701 mm

Fig. 6 Aspect map of the study area

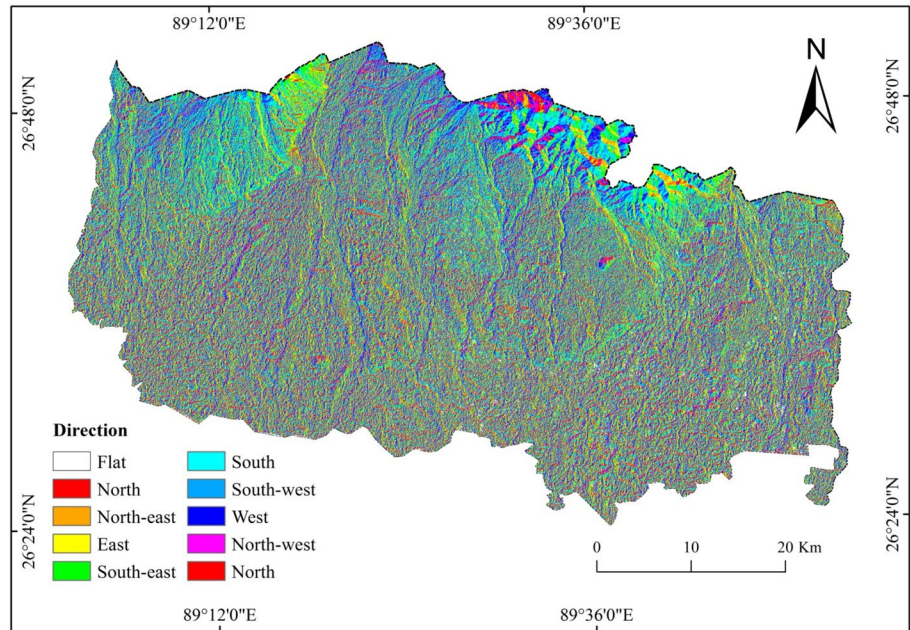
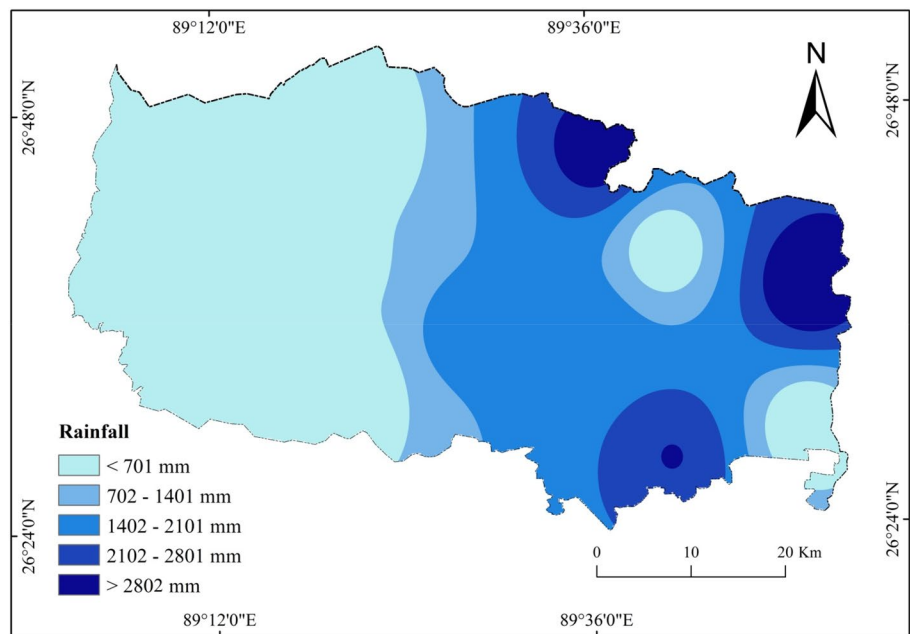


Fig. 7 Rainfall pattern in the study area

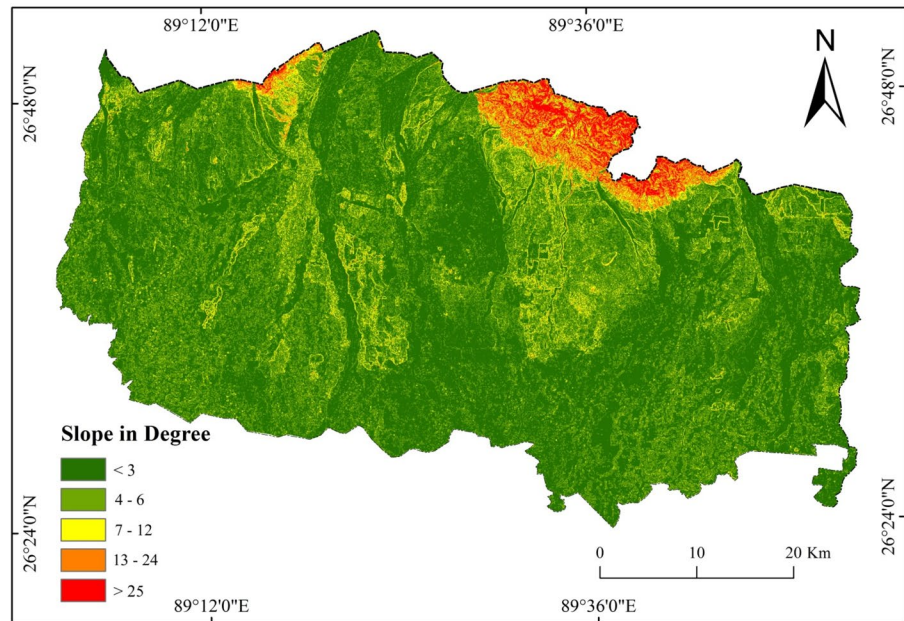


region indicates very high (46.50%), 702–1401 mm region moderate (12.68%), 1402–2101 mm region high (26.64%), 2102–2801 mm region low (9.18%) and > 2802 mm region exceptionally low (5.0%) groundwater potential in the study area. Heavy rainfall was recorded in the north, northeast, southeast region. Generally, it is believed that the infiltration rate and subsequently groundwater recharge will be more in the areas where higher amount of rainfall occurs. Therefore, higher weight is assigned to higher rainfall zones for delineating the potential zones of groundwater and vice versa (Table 6).

Slope

Runoff and infiltration are influenced by the area's slope. The runoff increases with a steeper slope (Gupta et al. 2018a, b). Due to the longer residence period for water to percolate, previous studies suggested that groundwater potentiality improves with gentle slope and low topographic elevation locations. Slant of a land is a significant boundary which impacts the water maintenance and power of invasion starting precipitation (Rahman et al. 2012). Extremely high groundwater potential is attributed to places with greater

Fig. 8 Slope map of the study area

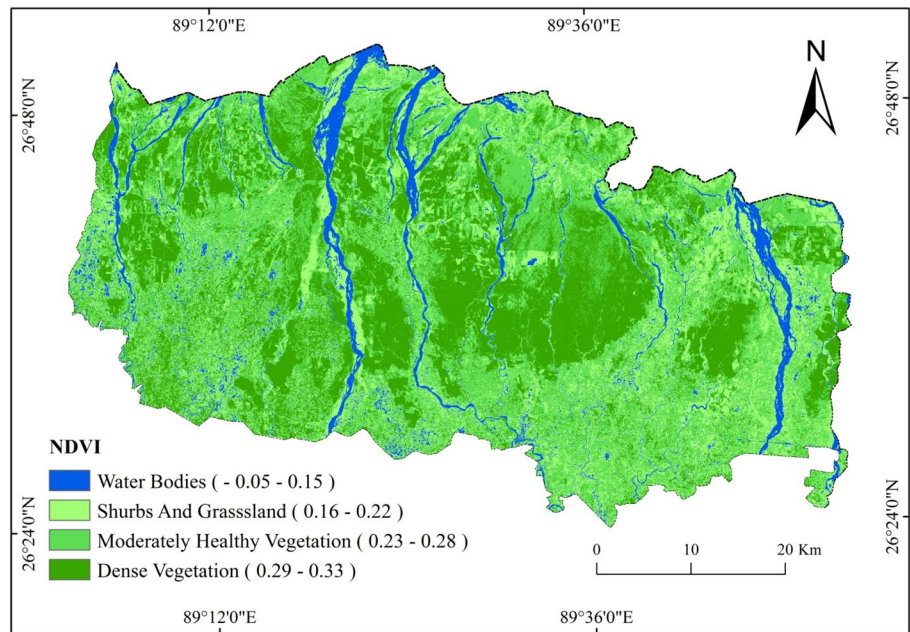


slope, since they typically have considerable runoff and poor penetration. Any location's geographical incline has a bearing on how surface water will run off, re-energize, and develop. There is always an inverse relationship between the infiltration of water and the degree of slope, since a steeper slope results in higher surface runoff and less groundwater recharge because there is insufficient time for the surface to percolate (Ghosh et al. 2016; Rajasekhar et al. 2019; Murmu et al. 2019). Aster Dem (30 m) was used to create the incline guide for the inquiry area, which was divided into five classes. The class having less worth is appointed higher position because of the practically level landscape, while the class having greatest worth is arranged as lower rank because of moderately high overflow. Less incline demonstrates low runoff and the other way around. Therefore, based on our study, the slope map has five classes, viz., level to gentle (<3°), moderate sloping (4°–6°), strong sloping (7°–12°), steep (13°–24°), and very steep (>25°) (Fig. 8). So, the <3° region has very high (62.53%), 4°–6° region high (26.95%), 7°–12° region moderate (6.16%), 13–24° region low (2.91%) and >25° region exceptionally low (1.45%) groundwater potential in the study area. The northern steep slope is considered to have a very low recharge, very high steep slope and no infiltration. However, a gentle slope is situated in the central-southern part of the map and the area has strong possibility to recharge the groundwater as well. All these categories were ranked based on earlier studies and groundwater availability given in (Table 6).

Normalized difference vegetation index (NDVI)

For monitoring vegetation dynamics at both regional and global scales, NDVI is a widely used indicator. The NDVI typically ranges from –1 to +1. There is a good chance that it is dense green vegetation if the NDVI value is close to +1. When the NDVI is close to 0, the area might even be urbanized because no greenery is there. This definition of NDVI produces a picture wherein the positive information indicates commonly open vegetation regions, while the negative qualities are regularly non-vegetation highlights. Like NDWI, NDVI has a scale of –1 to +1. The formula of $NDVI = (NIR - RED) / (NIR + RED)$ (Tucker 1979), where RED is for the visible red band (0.630–0.680 m) and NIR represents the near-infrared band (0.77–0.90 m). The NDVI is used as a proximate indicator of the presence of groundwater beneath the earth's surface, because areas with high vegetation are frequently found to have shallow groundwater levels (Patra et al. 2018). The NDVI of our study is arranged into four classes (Fig. 9) for the research area. The output of the thematic map of NDVI is grouped into four classes, such as water bodies, shrubs–grassland, moderately healthy vegetation, and dense healthy vegetation. Healthy vegetation and sufficient groundwater recharge appear to be related in a given area (Senapati and Das 2021). The dense vegetation area is very much susceptible to groundwater recharge and is close to the riverine area. More weight is assigned to dense healthy vegetation, whereas shrubs–grassland are given a moderate weight (Table 6) and the rest are given low weightage for the potentiality of groundwater. The water bodies

Fig. 9 NDVI pattern in the study area

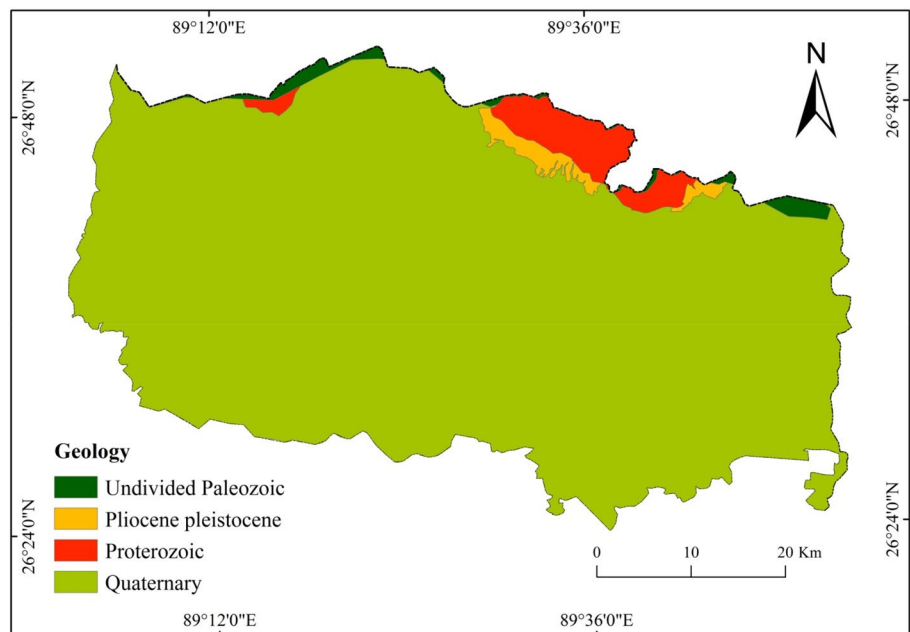


(between -0.05 and 0.15), which made up 6.04% of the area, shrub–grassland (between 0.16 – 0.22), which made up 12.47% of the area, moderately healthy vegetation (between 0.23 and 0.28), which made up 59.21% of the area, dense healthy vegetation (between 0.29 and 0.33), which made up 22.28% of the study area. About 6.04% region is excellent, 12.47% moderate, low 59.21% and 22.28% very low vegetation region. The dense healthy vegetation and moderately healthy vegetation are play good role in groundwater potentiality of our study area.

Geology

Since infiltration and runoff rate mostly depends on the porosity of rocks. The geological foundation of any place is another crucial component that regulates groundwater supply (Yeh et al. 2016; Abijith et al. 2020). The geological horizon affects both the occurrence and the flow of groundwater. It could hold water and permit simple water movement if it were porous and permeable. On the basis of geological map (Fig. 10), it was observed that the study area is covered in a variety of geological formations, including the

Fig. 10 Geology pattern in the study area



sub-Himalayan and Chalsa formation. These two formations are confined within the Himalayan arc. This formation is mainly characterized by alluvial fan geology, brown color topsoil, and yellow colored sediment weathering zone. The geological age of this formation is early Holocene to late Pleistocene. Based on the chronological order, the Paleozoic formation is found in the extreme north in a linear way. Subsequently, the next geological formation was Proterozoic formation which mainly spread along the Paleozoic formation in the north of the study area, whereas the Pleistocene formation covers near the Proterozoic formation in the north portion. However, most of the district is covered with undifferentiated Siwalik sediments (Plio-Pleistocene), followed by undifferentiated fluvial–glacial sediments, which were also deposited during the very recent Quaternary epoch, primarily distributed in the southern half and runs primarily from the western to the eastern section. The geology map is classified into five formations, i.e., undivided Paleozoic, Pliocene Pleistocene, Proterozoic and Quaternary. As a result, this Quaternary deposition of unconsolidated sediments is more conducive than others for the future development of groundwater (Aggarwal et al. 2019). The study area is tectonically active and faces many sediment depositions from rivers, and ultimately favors groundwater recharge and development. The Paleozoic formation is made up 0.12% of the area, Pleistocene formation 1.18%, Proterozoic formation 3.42%, and Quaternary 95.28%. As in earlier studies, high weightage is given to the Quaternary formation due to being highly favorable for groundwater.

Soil texture

Soil is the topmost layer above the earth that acts as a conduit for the percolation of water. Texture of the soil is a significant criterion to assess the physical state of the soil and is straightforwardly connected with soil properties such as design, porosity, grip and uniformity (McGarry 2006). The soil in this area differs from alluvial soil to dry and hard black clay. The permeability and water-holding capacity of the soil affect the rate of infiltration (Gupta et al. 2018a, b). The National Bureau of Soil Survey and Land Use Planning provided the soil texture map (NBSS & LUP). The soil type, which affects permeability, regulates the groundwater infiltration and retention rate. The finer the soil texture, the lower is the infiltration capacity, and as a result, less groundwater will be recharged; in contrast, the coarser the soil texture, the greater will be infiltration in the soil. The research region is separated into five different types: coarse loamy, umbric Dystrachrepts, fine loamy, aeric Haplaquepts, coarse loamy, typic Ustorthents, fine loamy, fluventic Ustochrept, coarse loamy, aquic Udifluvents, coarse loamy, aquic Ustifluvents, fine Fluvaquents, coarse loamy, typic Haplaquents, and coarse loamy, typic Fluvaquents, which are considered 9.03, 1.34, 18.82, 1.26, and 69.55% of the study area (Fig. 11). In the upper area in the north of Dooars, the soil is principally dark and clayey. This soil is reasonable for developing tea, which is a significant money harvest of this region. In the lower plain, the soil comprises of a combination of both mud, sand and coarse loamy. The lower alluvial soil area is prolific enough for crops like paddy, wheat, jute, potato, beats, oilseeds, sugarcane and so on to be developed. A huge number of waterways and streams begin from the sloping spaces of neighboring Bhutan and there is an organization of

Fig. 11 Soil texture pattern in the study area

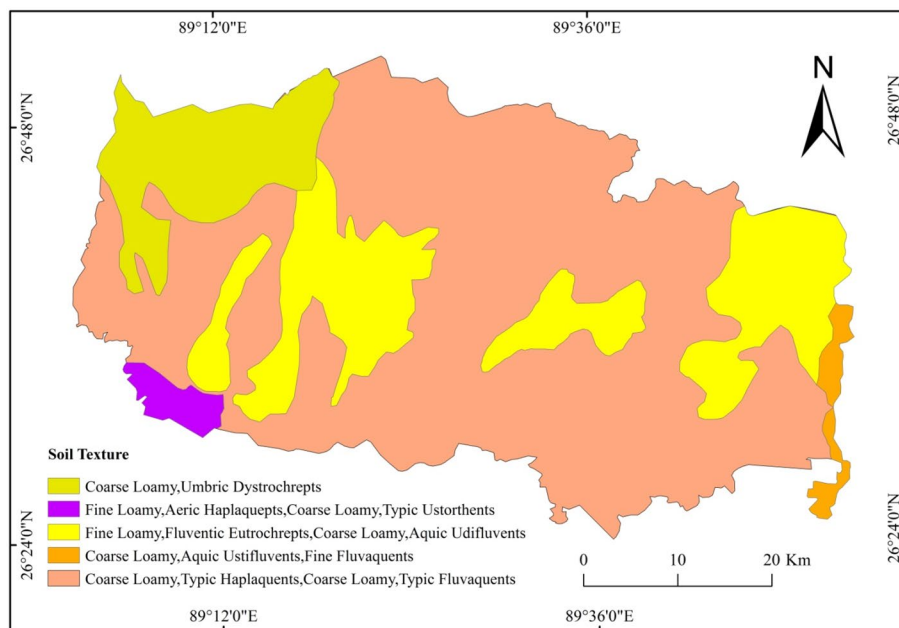
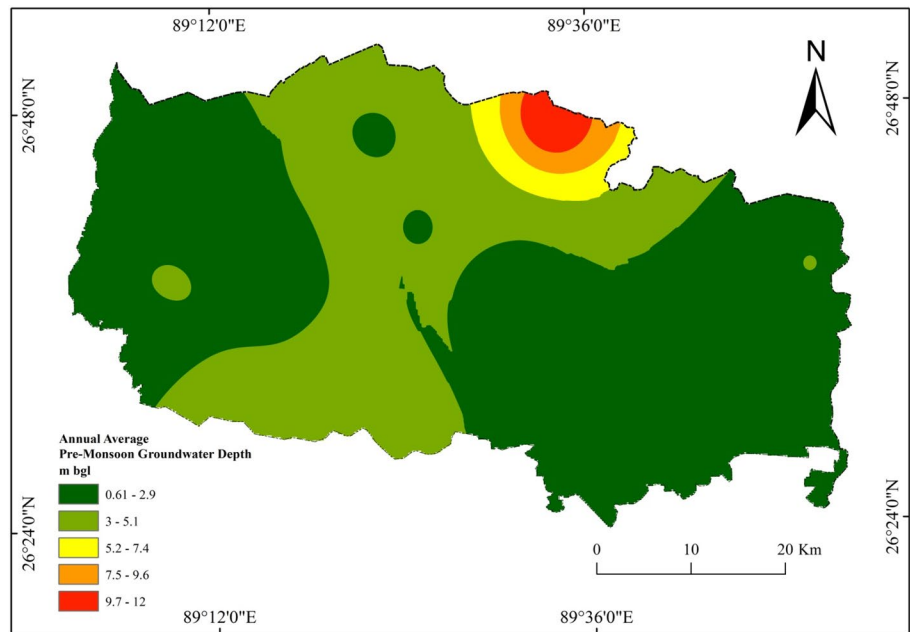


Fig. 12 Pattern of pre-monsoon annual (2018–2021) groundwater depth in the study area



streams befuddling the whole district. The significant streams are Teesta, Torsa, Jaldhaka, Kaljani, Raidak, Korotowa and Sankos. They are joined more modest streams like Dudua, Tasati, and Mujnai and so forth. The river frequently flood their banks keeping layers of prolific soil on the banks on one or the other side.

Pre-monsoon groundwater depth

To comprehend the annual effect, pre- and post-monsoon data paired with other data were also investigated. In April, groundwater recharge was assessed using pre-monsoon data collected during 2018–2021. During the study, this parameter was used for better identification of groundwater in our study area. In West Bengal, pre-rain storm checking is done during the long stretch of April relying upon the time

Fig. 13 Pattern of post-monsoon annual (2018–2021) groundwater depth in the study area

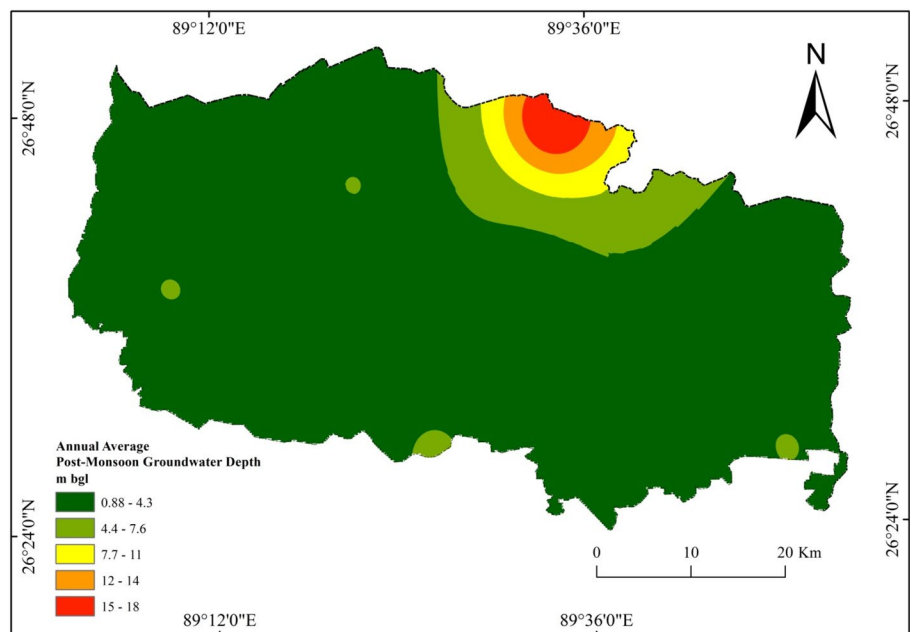


Table 7 Categories of groundwater potential zone

| Range | Groundwater potential | Area (%) | Area (Km ²) |
|---------|-----------------------|----------|-------------------------|
| 5–85 | Very poor | 3.7 | 116.03 |
| 85–138 | Poor | 7.1 | 222.66 |
| 138–187 | Moderate | 11.3 | 354.37 |
| 187–226 | Good | 27.4 | 859.26 |
| 226–272 | Excellent | 50.5 | 1583.68 |

frame for the beginning of the monsoon. Several well water depth heights are collected and calculated during the years. The average annual pre-monsoon groundwater depth map (Fig. 12) is taken to identify GWPZ. Patra et al. (2018) used 5 years' groundwater depth. Pre-monsoon water level data from 2018 to 2021 were used to depict the regional distribution of water levels and their classification under various ranges (Fig. 16a). The pre-monsoonal shower helped to recharge groundwater. However, groundwater flow will be lower and stay in the aquifer for longer during the pre-monsoon season (Kochhar et al. 2022). Water level information represents the spatial appropriation of water level and its classification under unique reaches. Fig. 12 shows the pattern of groundwater depth in pre-monsoon season during 2018–2021. The western and eastern parts of the study area have greatest groundwater depth varying from 0.61 m bgl to 0.29 m bgl. The second-most profound area, with a range of 3.00 m to 5.1 m bgl, is in the center of Alipurduar from north to south. The depth is moderate to very deep, varying from 5.2 to 12 m bgl, in the northern parts. Pre-monsoon water depth fluctuated annually between 0.39 m bgl and 20.41 m bgl during 2018–2019 and 2019–2021. High weightage is given to the less depth of pre-monsoon (0.61–0.29 m bgl), whereas the lowest weightage Table (6) is given to the very high depth (9.70–12.00 m bgl) of groundwater.

Post-monsoon groundwater depth

Aquifer material and rainfall pattern are primarily responsible for controlling post-monsoon groundwater depth. It is essential to appreciate the spatial difference of monsoonal rainfall and also how it impacts the increase in groundwater storage, thereby identifying the spatial distribution of groundwater zones (Fig. 13). The essential target is to document the reaction of groundwater system to the normal and man-made burdens of re-energizing and release boundaries regarding geography, environment, topography, land use design and hydrologic attributes. Using a graded steel tape, groundwater level in the well during both the pre- and post-monsoon seasons is measured (Shekhar and Jha 2022). Post-rainstorm information gathered during November mirrors the combined impact of groundwater re-energy. It is highly helpful to determine GWPZ using the average annual post-monsoon groundwater depth map (Patra et al. 2018). The spatio-temporal change in the post-monsoon groundwater level for 2018–2021 is depicted in Fig. 16b. In this way, to distinguish GWPZ, normal yearly post-storm groundwater profundity map is exceptionally valuable. The research area's average annual post-monsoon groundwater depth map is shown in Fig. 13. It is divided into five groups: (a)

Fig. 14 Land use and land cover map of the study area

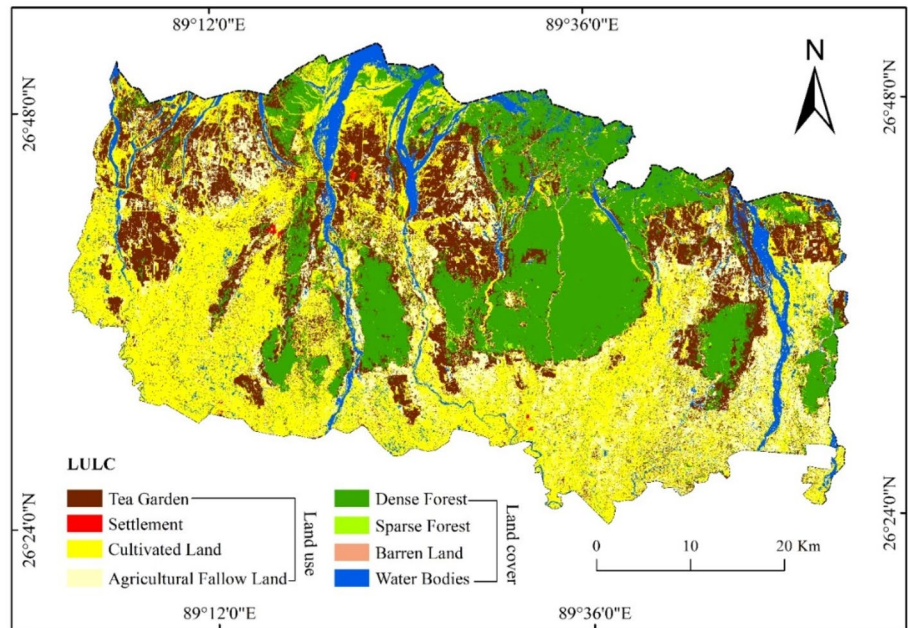
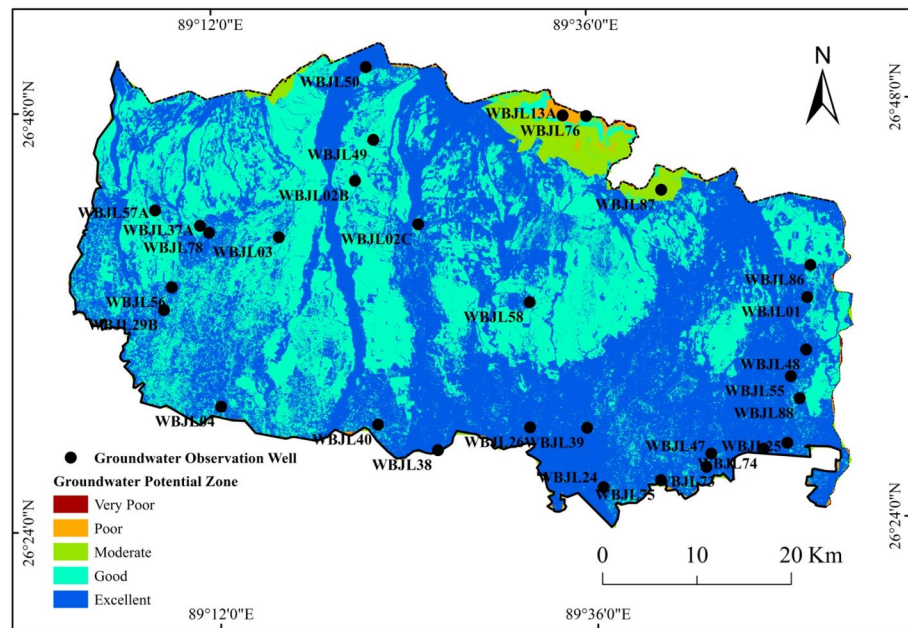


Fig. 15 Groundwater potential zone of the Alipurduar district



0.88–4.30 m bgl (88.19%), (b) 4.40–7.60 m bgl (10.12%), (c) 7.70 – 11.00 m bgl (4.16%), (d) 12.00–14.00 m bgl (2.29%) and (f) 15.00–18.00 m bgl (1.24%). The groundwater depth is shallow to almost shallow in the western, central, and eastern portions of the research region (0.88–4.3 m bgl). In contrast, the groundwater depth in the northern Buxa area ranges from moderate to very deep (4.4 to 18.00 m bgl). Between 2018–2019 and 2019–2021, the annual variation in water table depth ranged from 0.36 m bgl to 29.59 m bgl. High weightage is given to the less depth (0.88–4.30 m bgl),

whereas the lowest weightage (Table 6) is given to the very high depth (15.00– 18.00 m bgl) of groundwater. After the rainy season, the water storage in the subsurface soil and lower subsurface soil is better to influence the groundwater.

Land use and land cover (LULC)

The primary factor influencing the LULC in the research area is groundwater supplies, and it also plays a crucial part in the management of groundwater sustainably (Rajasekhar et al. 2019; Abijith et al. 2020). Studies on land use and land

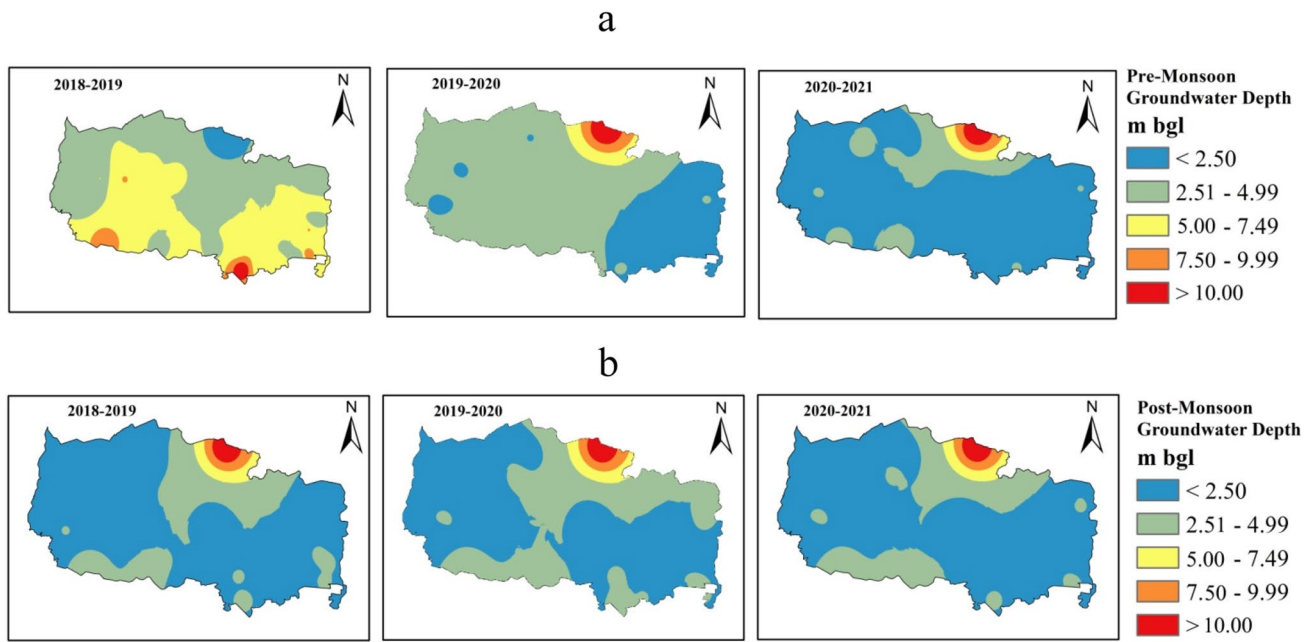


Fig. 16 Annual fluctuation of groundwater level in the study area. **a** Pre-monsoon (upper panel); **b** post-monsoon (lower panel)

cover are crucial for determining how much groundwater is needed and how it is being used in the groundwater potential zone. In comparison to other land uses like farmland and shrub land, bare land, which makes up about 50% of the basin area, has higher groundwater recharge rates (Albhaisi et al. 2013). Since irrigation increases the amount of water supplied to the fields and hence encourages groundwater recharge, crops were given a better score than shrub land and settlement land use (Roark and Healy 1998). According to Scanlon et al. (2005), the direction of water flow changes from lateral (discharge) to downward when rangelands are replaced by agricultural lands (recharge). On the other hand, urban land use has very low rankings in GWPZ's assessment, since it has low infiltration rates and capacities because impermeable surfaces predominate (Jat et al. 2009). The land use and land cover both significantly affect the groundwater recharge and discharge. Using the supervised classification technique, the Landsat 8 (30 m resolution) satellite picture was used to construct the land use/land cover map and was divided into eight groups (Fig. 14). Due to ample empty space for groundwater recharge, agricultural land has very good groundwater potential, whereas built-up areas have relatively low groundwater potential due to very little groundwater recharge. High groundwater potential zones are indicated by higher values, and vice versa. The LULC map defines that 12.39% of the area is tea garden, sparse forest 2.67%, dense forest 21.18%, cultivated land 28.99%, settlement 10.68%, water bodies 9.62%, barren land 3.19% and agricultural fallow land 11.428% respectively

(Table 6). The tea garden, dense forest with sparse vegetative area, cultivated land, and water bodies are influencing factors for groundwater recharge in the study area. The rank for tea garden, dense forest and cultivated land are assigned according to the prior study. The area is mostly covered with

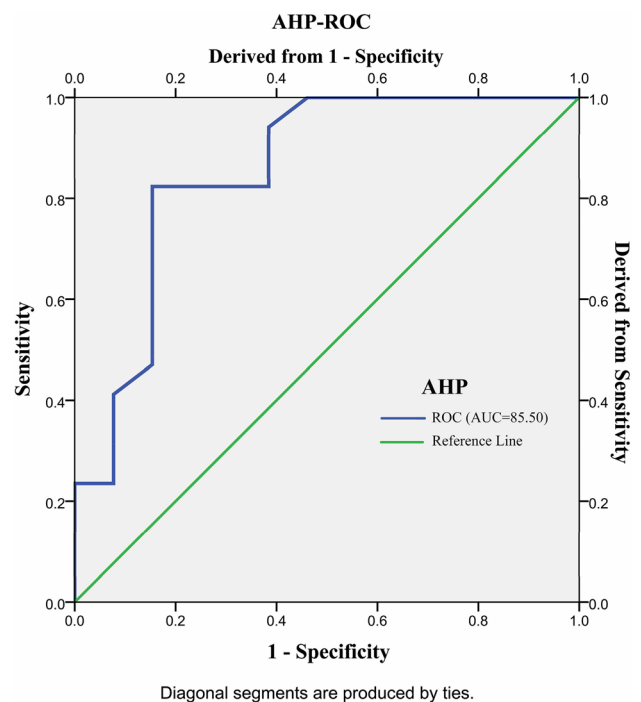


Fig. 17 ROC curve for groundwater potentiality zones map using AHP technique

these three mentioned areas and they are suitable for groundwater recharges. The presence of high forest cover and cultivated land helps in more penetration of water into the sub soil and which ultimately recharges the groundwater in the study area.

Groundwater potential zone

The groundwater potential for the research region was already determined with the help of a GIS-weighted overlay analysis and an AHP multi-influencing approach. A final groundwater potential map (Fig. 15) including the blocks of Madarihat, Kalchini, Kumargram, Falakata, and Alipurduar-I, II was produced through the examination of 12 thematic layers. The results obtained were divided into five groups (Table 7), ranging from very poor zone to excellent zones, using the index value determined by the above-described procedure. The research area's nearly flat terrain (in the district's south) offers the best environment for groundwater recharge. Slope, drainage density, geology, river network, and soil define the ultimate potential zone. Most people agree that rivers and other bodies of water are crucial for recharging groundwater. If there are too many rivers flowing in one location, the density of drainage rises, leading to heavy surface runoff and minimal infiltration. An excellent potential zone of about 50.5% (1583.68 km²) is found in the near river region and floodplain areas where the majority of alluvial sediments were found. Alluvium deposits favor the high infiltration of rainwater. High to very high NDWI, vicinity to rivers, low elevation, low to moderate drainage density, and coarse loamy soil regions fall under the excellent category. Similarly, the eastern and southern extreme portions of the potential map shows excellent potential zone, as high to moderate rainfall with coarse loamy soil will enforce the recharge of the groundwater. Forested land and the tea garden region fall under a good potential zone with 27.4% (859.26 km²) in the map. The vegetative ground with fine loamy soil, low elevation, and moderate rainfall is found to be a good zone. Favorable geology and fine loamy soil with forested land favor the recharge in a moderate zone. A moderate potential map is found in the northern portion of Kalchini block with 11.3% (354.37 km² area) extension. The poor zone is spotted in the northward site of the potential zone map. The zone is 7.1% and covers 222.66 km² of the map. Very poor potential zone is found in the extreme north of the map due to the high slope, Pleistocene age deposition, low recharge, and low drainage density, reflecting the very poor zone. The zone comprises 3.7% (very less) covering 116.03 km² of the map. The extreme north of Madarihat and Kalchini block falls under moderate–poor–very poor zone of groundwater. The other parts of the district are in the good and excellent conditions of the groundwater zone. In comparison to good and moderate GWPZ areas, poor

and very bad GWPZ areas have a lower discharge rate. The groundwater potential zone maps assist us in understanding the regional groundwater situation, so that we can plan and manage for long-term extraction and development.

Validation of groundwater potential zone

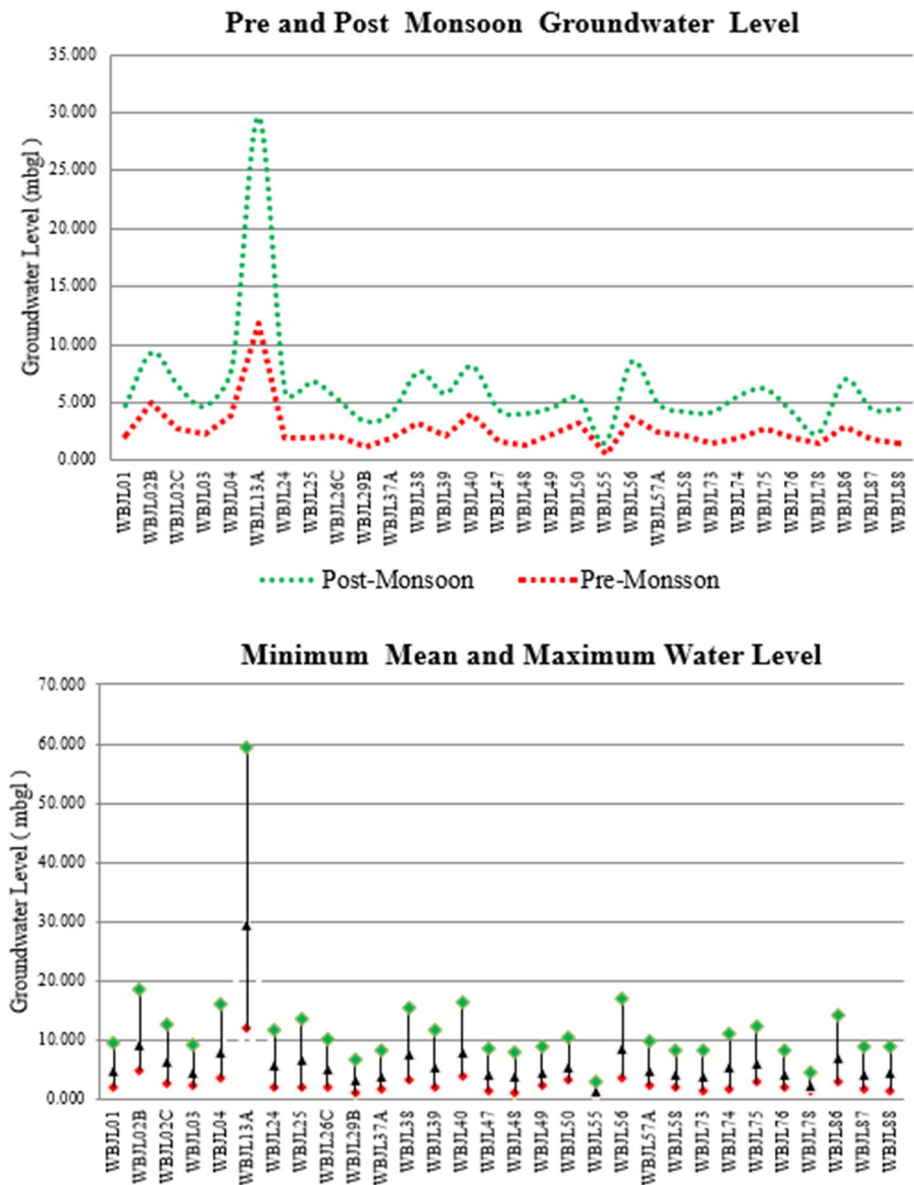
Science-based research needs to be verified. Using a receiver operating characteristic curve, the model is tested. The final groundwater potential zone is based on 30 true groundwater samples (Table 8) derived from the CGWB. The ROC curve was used in SPSS to assess map reliability. Pre-monsoon and post-monsoon water level depth information from the Center Ground Water Board (CGWB) for the most recent 3 years was taken (Fig. 16a and Fig. 16b). Around 30 checking wells were chosen (2021–22) in and around the review region and interpolated. The top left corner indicates a good performance level, while the curve in the bottom right corner indicates poor performance level. The area under the ROC curve (AUC) measures the ability of a parameter to discriminate between two diagnostic groupings (AUC). Greater AUC reflects good to very good validation between two levels. A blue line depicts the prediction rate in a visual representation (Fig. 17). In conclusion, the AHP/ANP technique is relatively very good (predictive) at 0.85 based on the final validation of the findings. Under the non-parametric assumption, the findings of AUC (0.855) and STD error (0.074) show that it has an accuracy of 85.5%, making it a reliable prediction model, indicating that the model's accuracy to designate the groundwater potential zone (GWPZ) is excellent. There are four ranges for AUC values: 0.5–0.6, 0.6–0.8 and 0.8–0.9 and five categories: very poor, poor, moderate, good, and excellent (Senapati and Das 2020, 2021; Arabameri et al. 2018). An overall picture of the local groundwater resources is provided by the geographical placement of classes and their equivalent potential condition in the various areas. Based on very poor, poor, medium, good, as well as excellent groundwater potential, these statistics enable the identification of different categories of groundwater potential areas. Therefore, the accurate final output map created by reliable GIS-based weighted overlays coupled with the AHP model is very consistent with the outcomes of the groundwater potential validation. Also, the real-time data show the good correlation with the result. Figure 18a calculates and depicts the water level's minimum, maximum, and mean values in the study area. The pre-monsoon and post-monsoon groundwater level is considered to check the extent of recharge in the research area. Increased water level during the post-monsoon and a minimal or low recharge zone during the pre-monsoon are shown in Fig. 18b.

Table 8 Accuracy assessment of GWPZ map with average groundwater level

| SL. no. | Observed well ID | Latitude (decimal degree) | Longitude (decimal degree) | Water level height (m bgl) | Groundwater level | Well location on GWPZs map | Raster value | Validation remarks | Binary value |
|---------|------------------|---------------------------|----------------------------|----------------------------|-------------------|----------------------------|--------------|--------------------|--------------|
| 1 | WBJL01 | 26.611012 | 89.829431 | 4.727 | Very shallow | Excellent | 235 | Agree | 0 |
| 2 | WBJL02B | 26.730871 | 89.350642 | 9.327 | Shallow | Excellent | 223 | Disagree | 1 |
| 3 | WBJL02C | 26.688203 | 89.417092 | 6.347 | Very shallow | Good | 215 | Disagree | 1 |
| 4 | WBJL03 | 26.678149 | 89.268471 | 4.66 | Very shallow | Good | 227 | Disagree | 1 |
| 5 | WBJL04 | 26.517486 | 89.20392 | 8.057 | Shallow | Good | 239 | Agree | 0 |
| 6 | WBJL13A | 26.788489 | 89.598111 | 12.683 | Moderate | Poor | 96 | Disagree | 0 |
| 7 | WBJL24 | 26.43361 | 89.608682 | 5.84 | Very shallow | Good | 226 | Disagree | 1 |
| 8 | WBJL25 | 26.472467 | 89.804846 | 6.827 | Shallow | Good | 225 | Agree | 0 |
| 9 | WBJL26C | 26.492216 | 89.531963 | 5.193 | Very shallow | Excellent | 243 | Agree | 0 |
| 10 | WBJL29B | 26.610499 | 89.144874 | 3.357 | Very shallow | Good | 239 | Disagree | 1 |
| 11 | WBJL37A | 26.69048 | 89.184776 | 4.127 | Very shallow | Good | 219 | Disagree | 1 |
| 12 | WBJL38 | 26.472686 | 89.43365 | 7.667 | Shallow | Good | 351 | Agree | 0 |
| 13 | WBJL39 | 26.490726 | 89.592489 | 5.763 | Very shallow | Excellent | 247 | Agree | 0 |
| 14 | WBJL40 | 26.497482 | 89.370411 | 8.147 | Shallow | Good | 231 | Agree | 0 |
| 15 | WBJL47 | 26.46366 | 89.723841 | 4.357 | Very shallow | Good | 244 | Disagree | 1 |
| 16 | WBJL48 | 26.560943 | 89.8271 | 4.023 | Very shallow | Excellent | 245 | Agree | 0 |
| 17 | WBJL49 | 26.769657 | 89.370946 | 11.749 | Moderate | Moderate | 223 | Agree | 0 |
| 18 | WBJL50 | 26.839193 | 89.364375 | 5.343 | Very shallow | Excellent | 233 | Agree | 0 |
| 19 | WBJL55 | 26.535888 | 89.810062 | 1.513 | Very shallow | Excellent | 240 | Agree | 0 |
| 20 | WBJL56 | 26.632092 | 89.153618 | 8.527 | Shallow | Good | 235 | Agree | 0 |
| 21 | WBJL57A | 26.705781 | 89.137253 | 4.853 | Very shallow | Good | 221 | Disagree | 1 |
| 22 | WBJL58 | 26.611686 | 89.534026 | 4.197 | Very shallow | Good | 220 | Disagree | 1 |
| 23 | WBJL73 | 26.451081 | 89.718505 | 4.15 | Very shallow | Excellent | 224 | Agree | 0 |
| 24 | WBJL74 | 26.467216 | 89.779384 | 5.553 | Very Shallow | Excellent | 243 | Agree | 0 |
| 25 | WBJL75 | 26.439402 | 89.669866 | 6.167 | Very shallow | Excellent | 234 | Agree | 0 |
| 26 | WBJL76 | 26.789403 | 89.573093 | 29.683 | Very deep | Very Poor | 220 | Agree | 1 |
| 27 | WBJL78 | 26.683584 | 89.194226 | 2.34 | Very shallow | Excellent | 237 | Agree | 0 |
| 28 | WBJL86 | 26.64163 | 89.833419 | 6.985 | Shallow | Excellent | 219 | Disagree | 1 |
| 29 | WBJL87 | 26.716438 | 89.676413 | 16.090 | Moderate | Moderate | 248 | Agree | 0 |
| 30 | WBJL88 | 26.514598 | 89.819051 | 4.447 | Very shallow | Good | 230 | Disagree | 1 |

less than 6.51 Very Shallow, 6.52–11.51 Shallow, 11.52–16.51 Moderate, 16.52–21.51 Deep, more than 21.52 Very deep

Fig. 18 a Minimum, mean, and maximum groundwater level (upper panel); **b** pre- and post-monsoon variation in groundwater level (lower panel)



Conclusion

Today, groundwater shortage has emerged as a serious global problem. In emerging nations like India, where the population is enormous, the situation is even worse due to massive groundwater extraction. In the district of Alipurduar, which is predominately agricultural—tea industry based, the current study was conducted on the groundwater potential zone utilizing GIS-based MCDM methodologies, specifically AHP. It is an agricultural area where availability of groundwater is important. Thus, modeling of the groundwater potential zone was done using the AHP and GIS techniques.

For the study, a total of 12 parameters were selected, viz., elevation, drainage density, NDWI, aspect, LULC,

rainfall, slope, NDVI, geology, soil, pre-monsoon groundwater depth, and post-monsoon groundwater depth to run the model in Alipurduar area. The final output based on the calculation of AHP reveals a total of five groundwater potential zones, i.e., 50.5% areas are excellent, 27.4% good, 11.3% moderate, 7.1% poor and 3.7% very poor. The southern portion consisting of active alluvial floodplain, agricultural tract, and forest area experiences maximum rainfall with low elevation slope, and the most important presence of subbasins with favorable soil condition increases the groundwater probability with favorable infiltration and recharge capacity. The northern portion, on the other hand, has poor groundwater potential due to its steep slope, irregular topography, extensive vegetation cover, and impenetrable hard geological

structure. Hence the result is that majority of the study area (50.5%) falls under excellent zone and 7.1% falls under poor potential zone. So a higher chance of potentiality was shown on the groundwater potential map. The results have been validated with ground-based data of 30 dug wells. Validation is done after the potential map by weight is assigned. The AHP technique generates a pairwise comparison matrix after taking into account the variables' preferences and how they relate to one another.

Due to the lack of any previous study on groundwater estimation in this Terai-Duars region, the current investigation has the potential to produce a revolutionary finding. Additionally, numerous other models (such as FR, WOE, MIF, CF, and so forth) may be used for future studies. Delineating the groundwater potential zone and comparing the results from different models were both strongly advised to assess the degree of accuracy. Other significant geographical and hydrological elements must be included to increase the degree of estimation for the groundwater probability map. In the area, it is possible to use artificial recharge techniques and a participative approach to increase the potentiality and groundwater table and ultimately prevent overexploitation.

This work has gained significance, since it is a groundbreaking effort to address irrigation concerns in the study area. As a result, this study significantly established a baseline assessment that future academics, regional planners, and policymakers can use to compare their findings to. Furthermore, this study implies that some topics may be the focus of future research. Further research is necessary, for instance, to definitively determine the spatial link between the irrigation hazard hotspots and overexploitation zone based on the field data. Additionally, difficulties with irrigation dangers, as well as their temporal, geographical, and seasonal fluctuations, are the other topics that will be of relevance in the future. Also the current study, which used the AHP and GIS techniques, produced a credible result and has broad applicability to other locations with comparable hydro-geographical circumstances, particularly in areas with mountainous terrain. Additionally, this research could help environmentalists and legislators create an effective plan for conserving watersheds and using groundwater sustainably. It can also serve as guidance for governmental organizations.

Acknowledgements The authors are sincerely thankful to the editor and anonymous reviewers for their valuable comments and suggestions. Moreover, the authors are grateful to different agencies for providing the required data free of cost. Central Ground Water Board and India-WRIS provided necessary data free of charge to us. The USGS provided the required satellite data. The district groundwater related information was provided by the State Water Resources & Development Department and SWID (Jalpaiguri), Government of West Bengal.

Data Availability Data will be made available on request.

References

- Abijith D, Saravanan S, Singh L, Jennifer JJ, Saranya T, Parthasarathy KSS (2020) GIS-based multi-criteria analysis for identification of potential groundwater recharge zones—a case study from Ponnaniyaru watershed, Tamil Nadu, India. *HydroResearch* 3:1–14
- Agarwal R, Garg PK (2016) Remote sensing and GIS based groundwater potential & recharge zones mapping using multi-criteria decision making technique. *Water Resour Manag* 30(1):243–260. <https://doi.org/10.1007/s11269-015-1159-8>
- Agarwal E, Agarwal R, Garg RD, Garg PK (2013) Delineation of groundwater potential zone: an AHP/ANP approach. *J Earth Syst Sci* 122(3):887–898. <https://doi.org/10.1007/s12040-013-0309-8>
- Aggarwal M, Saravanan S, Jacinth JJ, Abijith D (2019) Delineation of groundwater potential zones for hard rock region in Karnataka using AHP and GIS. *Springer, Cham* 2:265–283
- Agricultural contingency report. 2016, (annual report 2016–17), Department of Agriculture, Cooperation Farmers Welfare Ministry of Agriculture Farmers Welfare Government of India Kishi Bhawan, New Delhi. Retrieved from: https://agricoop.nic.in/sites/default/files/Annual_rpt_201617_E.pdf. Accessed 28 June 2022.
- Al-Abadi AM, Al-Temmeme AA, Al-Ghanimy MA (2016) A GIS-based combining of frequency ratio and index of entropy approaches for mapping groundwater availability zones at Badra–Al Al-Gharbi–Teeb areas. *Iraq Sustain Water Resour Manag* 2:265–283
- Albhaisi M, Brendonck L, Batelaan O (2013) Predicted impacts of land use change on groundwater recharge of the upper Berg catchment. *South Africa Water SA* 39:2
- Al-Djazouli M, Elmorabiti K, Rahimi A, Amellah O, Fadil O (2020) Delineating of groundwater potential zones based on remote sensing, GIS and analytical hierarchical process: A case of Waddai, eastern Chad. *GeoJournal* 66:876
- Aluko OE, Igwe O (2017) An integrated geomatics approach to groundwater potential delineation in the Akoko-Edo Area. *Nigeria Environ Earth Sci* 76(6):240. <https://doi.org/10.1007/s12665-017-6557-1>
- Aneesh R, Deka PC (2015) Groundwater potential recharge zonation of bengaluru urban district—a GIS based analytic hierarchy process (AHP) technique approach. *Int Adv Res J Sci Eng Technol.* 2:129–136
- Ansari S, Sheereen Z (2016) Socio-economic condition of tea garden worker in Alipurduar district, West Bengal. *IJRSS.* 6:6654
- Arabameri A, Pradhan B, Pourghasemi HR, Rezaei K (2018) Identification of erosion-prone areas using different multi-criteria decision-making techniques and GIS. *Geomatics* 9(1):1129–1155. <https://doi.org/10.1080/19475705.2018.1513084>
- Arulbalaji P, Padmalal D, Sreelash K (2019) GIS and AHP techniques based delineation of groundwater potential zones: a case study from Southern Western Ghats. *India Sci Rep.* <https://doi.org/10.1038/s41598-019-38567-x>
- Bagyaraj M, Ramkumar T, Venkatramanan S, Gurugnanam B (2013) Application of remote sensing and GIS analysis for identifying groundwater potential zone in parts of Kodaikanal Taluk, South India. *Front Earth Sci* 7(1):65–75. <https://doi.org/10.1007/s11707-012-0347-6>
- Barua S, Mukhopadhyay BP, Bera A (2021) Integrated assessment of groundwater potential zone under agricultural dominated areas in the western part of Dakshin Dinajpur district, West Bengal. *India Arab J Geosci* 14:1042. <https://doi.org/10.1007/s12517-021-07312-y>
- Bates BC, Kundzewicz ZW, Wu S, Palutikof JP (eds) (2008) Climate change and water. Technical paper of the intergovernmental panel on climate change, IPCC Secretariat, Geneva

- Bhunja GS (2020) An approach to demarcate groundwater recharge potential zone using geospatial technology. *Appl Water Sci* 10:138. <https://doi.org/10.1007/s13201-020-01231-1>
- Biswas S, Mukhopadhyay BP, Bera A (2020) Delineating groundwater potential zones of agriculture dominated landscapes using GIS based AHP techniques: a case study from Uttar Dinajpur district. *West Bengal Environ Earth Sci* 79(12):1–25. <https://doi.org/10.1007/s12665-020-09053-9>
- Bonilla Valverde JP, Blank C, Roidt M, Schneider L, Stefan C (2016) Application of a gis multi-criteria decision analysis for the identification of intrinsic suitable sites in costa rica for the application of managed aquifer recharge (mar) through spreading methods. *Water* 8(9):391. <https://doi.org/10.3390/w8090391>
- CGWB (2019) National compilation on dynamic ground water resources of India, 2017, Central Ground Water Board, Department of Water Resources, RD & GR. Ministry of Jal Shakti, Government of India, Faridabad. Retrieved from: <http://cgwb.gov.in/GW-Assessment/GWRA-2017-National-Compilation.pdf>. Accessed 1 May 2022.
- Chenini I, Mammou AB, El May M (2010) Groundwater recharge zone mapping using GIS-based multi-criteria analysis: a case study in Central Tunisia (Maknassy Basin). *Water Resource Manag* 24(5):921–939. <https://doi.org/10.1007/s11269-009-9479-1>
- Chowdhury A, Jha MK, Chowdary VM, Mal BC (2009) Integrated remote sensing and GIS-based approach for assessing groundwater potential in West Medinipur district, West Bengal. *India. Int J Remote Sens* 30(1):231e250
- Council D, Program DS (2010) Measuring the depletion of groundwater resources worldwide. In: Walker L (ed) *Science News*. Sacramento, CA
- CWC and CGWB (2016) A 21st Century Institutional Architecture for India's Water Reforms. Retrieved from: http://cgwb.gov.in/INTRA-CGWB/Circulars/Report_on_Restructuring_CWC_CGWB.pdf. Accessed 11 June 2022.
- Das M, Ashok N, Bishnupriya D, Om V (2018) Groundwater quality assessment and mapping using multivariate statistics and analytic hierarchy process in Bhubaneswar city, Odisha. *India Inter J Water* 12:195–207. <https://doi.org/10.1504/IJW.2018.093668>
- Dey S, Shukla UK, Mehrishi P, Mall RK (2021) Appraisal of groundwater potentiality of multilayer alluvial aquifers of the Varuna river basin, India, using two concurrent methods of MCDM. *Environ Dev Sustain*. <https://doi.org/10.1007/s10668-021-01400-5>
- Do P, Florke M (2005) Global-scale estimation of diffuse groundwater recharge. In: Din M (ed) *Frankfurt hydrology paper 03*. Institute of Physical Geography, Frankfurt University, Germany
- Ebrahimi H, Ghazavi R, Karimi H (2016) Estimation of groundwater recharge from the rainfall and irrigation in an arid environment using inverse modelling approach and RS. *Water Resour Manag* 30(6):1939–1951. <https://doi.org/10.1007/s11269-016-1261-6>
- GhorbaniNejad S, Falah F, Daneshfar M, Haghizadeh A, Rahmati O (2017) Delineation of groundwater potential zones using remote sensing and GIS based data-driven models. *Geocarto Int* 32(2):167–187. <https://doi.org/10.1080/10106049.2015.1132481>
- Ghosh PK, Bandyopadhyay S, Jana NC (2016) Mapping of groundwater potential zones in hard rock terrain using geoinformatics: a case of Kumari watershed in gal. *Model Earth Syst Environ* 2(1):1. <https://doi.org/10.1007/s40808-015-0044-z>
- Godebo TR (2005) Application of remote sensing and GIS for geological investigation and groundwater potential zone identification, southeastern Ethiopian plateau, Bale Mountains and the surrounding areas. Addis Ababa University. Retrieved from: <http://etd.aau.edu.et/handle/123456789/7948>. Accessed 13 May 2022.
- Greenbaum D (1992) Structural influences on the occurrence of groundwater in SE Zimbabwe. *Geol Soc Lond Spec Publ* 66(1):77–85. <https://doi.org/10.1144/GSL.SP.1992.066.01.04>
- Gumma MK, Pavelic P (2013) Mapping of groundwater potential zones across Ghana using remote sensing, geographic information systems, and spatial modeling. *Environ Monit Assess* 185(4):3561–3579. <https://doi.org/10.1007/s10661-012-2810-y>
- Gupta SK, Deshpande RD (2004) Water for India in 2050: first-order assessment of available options. *Curr Sci* 86(9):1216–1224
- Gupta D, Yadav S, Tyagi D (2018a) Tomar L Multi-Criteria Decision Analysis for Identifying of Groundwater Potential Sites. *Haridwar* 3:9–15
- Guru B, Seshan K, Bera S (2017) Frequency ratio model for groundwater potential mapping and its sustainable management in cold desert. *India J King Saud Univ Sci* 29(3):333–347. <https://doi.org/10.1016/j.jksus.2016.08.003>
- Hossein A, Ardakani H, Ekhtesasi MR (2016) Groundwater potentiality through analytic hierarchy process (AHP) using remote sensing and geographic information system (GIS). *Jgeope* 6:75–88
- IPCC (2018) *Global Warming of 1.5°C. An IPCC Special Report on the impacts of global warming of 1.5°C above pre-industrial levels and related global greenhouse gas emission pathways, in the context of strengthening the global response to the threat of climate change, sustainable development, and efforts to eradicate poverty* [Masson-Delmotte, V., P. Zhai, H.-O. Pörtner, D. Roberts, J. Skea, P.R. Shukla, A. Pirani, W. Moufouma-Okia, C. Péan, R. Pidcock, S. Connors, J.B.R. Matthews, Y. Chen, X. Zhou, M.I. Gomis, E. Lonnoy, T. Maycock, M. Tignor, and T. Waterfield (eds.)]. In Press.
- IPCC (2001) *Climate Change 2001. Synthesis Report. IPCC Third Assessment Report (TAR): A Contribution of Working Groups I, II, and III to the Third Assessment Report of the Intergovernmental Panel on Climate Change*. Ippc, 409.
- Ibrahim-Bathis K, Ahmed SA (2016) Geospatial technology for delineating groundwater potential zones in Doddahalla watershed of Chitradurga district, India. *Egypt J Remote Sens Sp Sci* 19:223–234. <https://doi.org/10.1016/j.ejrs.2016.06.002>
- Ishizaka A, Labib A (2011) Review of the main developments in the analytic hierarchy process. *Expert Syst Appl* 38(11):14336–14345. <https://doi.org/10.1016/j.eswa.2011.04.143>
- Jaiswal RK, Mukherjee S, Krishnamurthy J, Saxena R (2003) Role of remote sensing and GIS techniques for generation of groundwater prospect zones towards rural development approach. *Int J Remote Sens* 24(5):993e1008
- Jasrotia AS, Kumar A, Singh R (2016) Integrated remote sensing and GIS approach for delineation of groundwater potential zones using aquifer parameters in Devak and Rui watershed of Jammu and Kashmir. *India Arabian J Geosci* 9(4):1–15. <https://doi.org/10.1007/s12517-016-2326-9>
- Jat M, Khare D, Garg P (2009) Urbanization and its impact on groundwater: a remote sensing and GIS-based assessment approach. *Environmentalist* 29:17–32. <https://doi.org/10.1007/s10669-008-9176-2>
- Jha MK, Chowdary VM, Chowdhury A (2010) Groundwater assessment in Salboni Block, West Bengal (India) using remote sensing, geographical information system and multi-criteria decision analysis techniques. *Hydrogeol J* 18(7):1713–1728. <https://doi.org/10.1007/s10040-010-0631-z>
- Kochhar A, Singh H, Sahoo S et al (2022) Prediction and forecast of pre-monsoon and post-monsoon groundwater level: using deep learning and statistical modelling. *Model Earth Syst Environ* 8:2317–2329. <https://doi.org/10.1007/s40808-021-01235-z>
- Krishnamurthy J, Srinivas G (1995) Role of geological and geomorphological factors in groundwater exploration: a study using IRS LISS data. *Int J Remote Sens* 16(14):2595–2618. <https://doi.org/10.1080/01431169508954579>
- Krishnamurthy J, Venkatesa Kumar N, Jayaraman V, Manivel M (1996) An approach to demarcate ground water potential zones through remote sensing and a geographical information system. *Int J*

- Remote Sens 17(10):1867–1884. <https://doi.org/10.1080/0143169608948744>
- Kumar SS, Shruti K, Kant MS (2017) Delineation of groundwater potential zone using geospatial techniques for shimla city, himachal pradesh (India). IJSRD Inter J Sci Res. 50:665
- Kundzewicz ZW et al (2007) Freshwater resources and their management. In Parry ML, (eds) Climate change 2007: impacts, adaptation and vulnerability. Contribution of working group II to the fourth assessment report of the intergovernmental panel on climate change. Cambridge University Press Cambridge, UK
- Lee S, Lee CW (2015) Application of decision-tree model to groundwater productivity-potential mapping. Sustainability 7(10):13416–13432. <https://doi.org/10.3390/su71013416>
- Lee S, Hong SM, Jung HS (2017) GIS-based groundwater potential mapping using artificial neural network and support vector machine models: the case of Boryeong city in Korea. Geocarto Int. <https://doi.org/10.1080/10106049.2017.1303091>
- Machiwal D, Jha MK, Mal BC (2011) Assessment of groundwater potential in a semi-arid region of India using remote sensing, GIS and MCDM techniques. Water Resour Manag 25(5):1359–1386. <https://doi.org/10.1007/s11269-010-9749-y>
- Madani A, Niyazi B (2015) Groundwater potential mapping using remote sensing techniques and weights of evidence GIS model: a case study from Wadi Yalamlam basin, Makkah Province. Western Saudi Arabia Environ Earth Sci 74(6):5129–5142. <https://doi.org/10.1007/s12665-015-4524-2>
- Madrucci V, Taioli F, de Araújo CC (2008) Groundwater favorability map using GIS multicriteria data analysis on crystalline terrain, Sao Paulo. J Hydrol 357(3):153–173. <https://doi.org/10.1016/j.jhydrol.2008.03.0260>
- Magesh NS, Chandrasekar N, JP (2012) Delineation of groundwater potential zones in Theni district, Tamil Nadu, using remote sensing, GIS and MIF techniques. Geosci Front 3(2):189–196. <https://doi.org/10.1016/j.gsf.2011.10.007>
- Mahmoud SH, Alazba AA, Amin MT (2014) Identification of Potential Sites for Groundwater Recharge Using a GIS-Based Decision Support System in Jazan Region-Saudi Arabia. Water Resour Manag 28(10):3319–3340. <https://doi.org/10.1007/s11269-014-0681-4>
- Malczewski J (2006) GIS-based multicriteria decision analysis: a survey of the literature. Int J Geogr Inf Sci 20(7):703–726. <https://doi.org/10.1080/13658810600661508>
- Mallick J, Singh CK, Al-Wadi H, Ahmed M, Rahman A, Shashtri S, Mukherjee S (2015) Geospatial and geostatistical approach for groundwater potential zone delineation. Hydrol Process 29(3):395–418. <https://doi.org/10.1002/hyp.10153>
- McFEETERS SK (1996) The use of the normalized difference water index (ndwi) in the delineation of open water features. Int J Remote Sens 17(7):1425–1432. <https://doi.org/10.1080/0143169608948714>
- McGarry D (2006) A Methodology of Visual-soil Field Assessment Tool to Support, Enhance, and Contribute to the LADA Program. Food and Agriculture Organization, Rome, Italy. Retrieved from: <https://www.fao.org/3/i6362e/i6362e.pdf>. Accessed 27 May 2022.
- Mogaji K, Omosuyi G, Adelusi A, Lim H (2016) Application of GIS-based evidential belief function model to regional groundwater recharge potential zones mapping in hardrock geologic terrain. Environ Process 3:93–123
- Moges DM, Bhat H, Thrivikramji KP (2019) Investigation of groundwater resources in highland Ethiopia using a geospatial technology. Model Earth Syst Environ. <https://doi.org/10.1007/s40808-019-00603-0>
- Mukherjee P, Singh CK, Mukherjee S (2012) Delineation of groundwater potential zones in arid region of India-a remote sensing and gis approach. Water Resour Manag 26(9):2643–2672. <https://doi.org/10.1007/s11269-012-0038-9>
- Murmu P, Kumar M, Lal D, Sonkerb I, Singh SK (2019) Delineation of groundwater potential zones using geospatial techniques and analytical hierarchy process in Dumka district. Groundwater Sustain Dev, Jharkhand, India. <https://doi.org/10.1016/j.gsd.2019>
- Murthy KSR (2000) Ground water potential in a semi-arid region of Andhra Pradesh - a geographical information system approach. Int J Remote Sens 21(9):1867–1884. <https://doi.org/10.1080/014311600209788>
- Nag SK, Ghosh P (2013) Delineation of groundwater potential zone in Chhatna Block, Bankura District, West Bengal, India using remote sensing and GIS techniques. Environ Earth Sci 70(5):2115–2127. <https://doi.org/10.1007/s12665-012-1713-0>
- Nagarajan M, Singh S (2009) Assessment of groundwater potential zones using GIS technique. J Indian Soc Remote Sens 37(1):69–77. <https://doi.org/10.1007/s12524-009-0012-z>
- Naghbi SA, Pourghasemi HR, Dixon B (2016) GIS-based groundwater potential mapping using boosted regression tree, classification and regression tree, and random forest machine learning models in Iran. Environ Monit Assess 188(1):44. <https://doi.org/10.1007/s10661-015-5049-6>
- Nampak H, Pradhan B, Manap MA (2014) Application of GIS based data driven evidential belief function model to predict groundwater potential zonation. J Hydrol 513:283–300. <https://doi.org/10.1016/j.jhydrol.2014.02.053>
- Patra S, Mishra P, Mahapatra SC, Mithun SK (2016) Modelling impacts of chemical fertilizer on agricultural production: a case study on Hooghly district, West Bengal. India Model Earth Syst Environ 2(4):180. <https://doi.org/10.1007/s40808-016-0223-6>
- Patra S, Mishra P, Mahapatra SC (2018) Delineation of groundwater potential zone for sustainable development: a case study from Ganga alluvial plain covering Hooghly district of India using remote sensing, geographic information system and analytic hierarchy process. J Clean Prod 172:2485–2502
- Pourtaghi ZS, Pourghasemi HR (2014) GIS-based groundwater spring potential assessment and mapping in the Birjand Township, southern Khorasan Province. Iran Hydrogeol J 22(3):643–662. <https://doi.org/10.1007/s10040-013-1089-6>
- Prasad RK, Mondal NC, Banerjee P, Nandakumar MV, Singh VS (2008) Deciphering potential groundwater zone in hard rock through the application of GIS. Environ Geol 55(3):467–475. <https://doi.org/10.1007/s00254-007-0992-3>
- Preeja KR, Joseph S, Thomas J, Vijith H (2011) Identification of groundwater potential zones of a tropical river basin (Kerala, India) using remote sensing and GIS techniques. J Indian Soc Remote Sens 39(1):83e94
- Rahman MA, Rusteberg B, Gogu RC, Lobo Ferreira JP, Sauter M (2012) A new spatial multi-criteria decision support tool for site selection for implementation of managed aquifer recharge. J Environ Manage 30(99):61–75. <https://doi.org/10.1016/j.jenvman.2012.01.003>
- Rajasekhar M, Sudarsana Raju G, Sreenivasulu Y, Raju RS (2019) Delineation of groundwater potential zones in semi-arid region of Jilledubanderu river basin, Anantapur district, Andhra Pradesh, India using fuzzy logic, AHP and integrated fuzzy-AHP approaches. Hydro Res. 10:554
- Rao S (2006) N (2006) Groundwater potential index in a crystalline terrain using remote sensing data. Environ Geol 50:1067–1076. <https://doi.org/10.1007/s00254-006-0280-7>
- Razavi-Termeh S, Sadeghi-Niaraki A, Choi S (2019) Groundwater Potential Mapping Using an Integrated Ensemble of Three

- Bivariate Statistical Models with Random Forest and Logistic Model Tree Models. *Water* 11:1596
- Report of the Ground Water Resource Estimation Committee (2009) Ministry of Water Resources Government of India, New Delhi. Retrieved from: <http://cgwb.gov.in/documents/gec97.pdf>. Accessed 22 June 2022.
- Roark D, Healy D (1998) Quantification of Deep Percolation from Two Flood-Irrigated Alfalfa Fields, Roswell Basin, New Mexico; USGS Water Resources Investigation Report 98–4096; U.S. Department of the Interior, U.S. Geological Survey: Albuquerque, NM, USA, 32p. Available online: <https://pubs.usgs.gov/wri/1998/4096/report.pdf> Accessed on 30 Dec 2022
- Rodell M, Velicogna I, Famiglietti JS (2009) Satellite-based estimates of groundwater depletion in India. *Nature* 460(7258):999–1002
- Rudra K, Mukherjee SS, Mukhopadhyay UK, Gupta D (2017) State of environment report, West Bengal, 2016. Saraswaty Press Ltd, West Bengal Pollution Control Board. Retrieved from: https://www.wbpcb.gov.in/writereaddata/files/SOE_Report_2016_1.pdf. Accessed 17 June 2022.
- Saaty TL (1980) *The Analytic Hierarchy Process: Planning, Priority Setting, Resource Allocation*, McGraw-Hill, New York
- Saaty TL (1990) How to make a decision: the analytic hierarchy process. *Eur J Oper Res* 48(1):9–26. [https://doi.org/10.1016/0377-2217\(90\)90057-1](https://doi.org/10.1016/0377-2217(90)90057-1)
- Saaty TL (2008) Decision making with the analytic hierarchy process. *Int J Serv Sci* 1(1):83
- Saha D, Dhar YR, Vittala SS (2010) Delineation of groundwater development potential zones in parts of marginal Ganga Alluvial Plain in South Bihar. *Eastern India Environ Monit Assess* 165(1):179–191. <https://doi.org/10.1007/s10661-009-0937-2>
- Sahoo S, Dhar A, Kar A, Ram P (2017) Grey analytic hierarchy process applied to effectiveness evaluation for groundwater potential zone delineation. *Geocarto Int*. 32(11):1188–1205. <https://doi.org/10.1080/10106049.2016.1195888>
- Sajad M, Mohammad B, Rather Dr G, Durdanah M (2021) Groundwater potential zonation using integration of remote sensing and ahp/anp approach in north kashmir, western himalaya. *India. Rem Sens Land*. 5:41–58
- Sar N, Khan A, Chatterjee S et al (2015) Hydrologic delineation of ground water potential zones using geospatial technique for Kelgghai river basin. *India Model Earth Syst Environ* 1:25. <https://doi.org/10.1007/s40808-015-0024-3>
- Saraf AK, Choudhury PR (1998) Integrated remote sensing and GIS for groundwater exploration and identification of artificial recharge sites. *Int J Remote Sens* 19(10):1825–1841. <https://doi.org/10.1080/014311698215018>
- Saranya T, Saravanan S (2020) Groundwater potential zone mapping using analytical hierarchy process (AHP) and GIS for Kancheepuram District, Tamilnadu. *India Model Earth Syst Environ* 6:1105–1122. <https://doi.org/10.1007/s40808-020-00744-7>
- Scanlon B, Reedy R, Stonestrom D, Prudic D, Dennehy K (2005) Impact of land use and land cover change on groundwater recharge and quality in the southwestern US. *Glob Chang Biol* 11:1577–1593
- Schultz GA, Engman ET (2012) *Remote sensing in hydrology and water management*. Springer Sci. <https://doi.org/10.1007/978-3-642-59583-7>
- Senanayake IP, Dissanayake DMDOK, Mayadunna BB, Weerasekera WL (2016) An approach to delineate groundwater recharge potential sites in Ambalantota, Sri Lanka using GIS techniques. *Geosci Front* 7(1):115–124. <https://doi.org/10.1016/j.gsf.2015.03.002>
- Senapati U, Das TK (2020) Assessment of potential land degradation in Akarsha Watershed, using GIS and multi-influencing factor technique. In: Shit P (ed) *Gully erosion studies from India and surrounding regions*. Advances in Science, Technology Innovation, Cham Newyork
- Senapati U, Das TK (2021) Assessment of basin-scale groundwater potentiality mapping in drought-prone upper Dwarakeshwar River basin, West Bengal, India, using GIS-based AHP techniques. *Arab J Geosci* 14(11):1–22. <https://doi.org/10.1007/s12517-021-07316-8>
- Sener E, Davraz A, Ozcelik M (2005) An integration of GIS and remote sensing in groundwater investigations: A case study in Burdur Turkey. *Hydrogeol J* 13(5–6):826–834. <https://doi.org/10.1007/s10040-004-0378-5>
- Shekhar S, Jha M (2022) Groundwater level prediction of Varanasi wells during pre-monsoon and post-monsoon using intelligence approach. *Arab J Geosci* 15:88. <https://doi.org/10.1007/s12517-021-08875-6>
- Shekhar S, Pandey AC (2015) Delineation of groundwater potential zone in hard rock terrain of India using remote sensing, geographical information system (GIS) and analytic hierarchy process (AHP) techniques. *Geocarto Int* 30(4):402–421. <https://doi.org/10.1080/10106049.2014.894584>
- Sikdar PK, Chakraborty S, Adhya E, Paul PK (2004) Land use/Land cover changes and groundwater potential zoning in and around Raniganj coal mining area, Bardhaman District, West Bengal-A GIS and Remote Sensing Approach. *J. Spatial Hydrol.* 4:776
- Singh SK, Kanga S, Mishra S (2017) Delineation of Groundwater Potential Zone Using GeospatialTechniques for Shimla City, Himachal Pradesh (India). *IJSRD - International Journal for Scientific Research & Development* 5(0)
- Srivastava PK, Bhattacharya AK (2006) Groundwater assessment through an integrated approach using remote sensing, GIS and resistivity techniques: a case study from a hard rock terrain. *Int J Remote Sens* 27(20):4599–4620. <https://doi.org/10.1080/01431160600554983>
- Taylor RG, Todd MC, Kongola L, Maurice L, Nahozya E, Sanga H, MacDonald A (2013) Evidence of the dependence of groundwater resources on extreme rainfall in East Africa. *Nat Clim Change* 3(4):374–378. <https://doi.org/10.1038/nclimate1731>
- Thapa R, Gupta S, Guin S, Kaur H (2017) Assessment of groundwater potential zones using multi-influencing factor (MIF) and GIS a case study from Birbhum district, West Bengal. *Appl. Water Sci.* 7:4117–4131. <https://doi.org/10.1007/s13201-017-0571-z>
- Tucker CJ (1979) Red and photographic infrared linear combinations for monitoringvegetation. *Remote Sens Environ* 8:127–150. [https://doi.org/10.1016/0034-4257\(79\)90013-0](https://doi.org/10.1016/0034-4257(79)90013-0)
- Yeh H, Cheng Y, Lin H, Lee C (2016) Mapping groundwater recharge potential zone using a GIS approach in Hualian River, Taiwan. *Sustain Environ Res.* 6(1):33–43 <https://doi.org/10.1016/j.serj.2015.09.005>
- Zaidi FK, Nazzal Y, Ahmed I, Naeem M, Jafri MK (2015) Identification of potential artificial groundwater recharge zones in North-western Saudi Arabia using GIS and Boolean logic. *J African Earth Sci* 111:156–169. <https://doi.org/10.1016/j.jafrearsci.2015.07.008>

Publisher's Note Springer Nature remains neutral with regard to jurisdictional claims in published maps and institutional affiliations.

Springer Nature or its licensor (e.g. a society or other partner) holds exclusive rights to this article under a publishing agreement with the author(s) or other rightsholder(s); author self-archiving of the accepted manuscript version of this article is solely governed by the terms of such publishing agreement and applicable law.